การแยกไอโซฟลาโวนจากสารสกัดจากกากถั่วเหลือง
โดยโครมาโตกราฟีแบบของเหลวสมรรถนะสูง

นางสาว ณัฐดา จูงหัตถการสาธิต

วิทยานิพนธ์นี้เป็นส่วนหนึ่งของการศึกษาตามหลักสูตรปริญญาวิศวกรรมศาสตรมหาบัณฑิต
สาขาวิชา วิศวกรรมเคมี ภาควิชา วิศวกรรมเคมี
คณะวิศวกรรมศาสตร์ จุฬาลงกรณ์มหาวิทยาลัย
ปีการศึกษา 2545
ISBN 974-17-0959-5

SEPARATION OF ISOFLAVONES FROM SOYBEAN FLAKE EXTRACTS BY HIGH PERFORMANCE LIQUID CHROMATOGRAPHY

Ms. Nattada Junghuttakarnsatit

A Thesis Submitted in Partial Fulfillment of the Requirements
for the Degree of Master of Engineering in Chemical Engineering
Department of Chemical Engineering
Faculty of Engineering
Chulalongkorn University
Academic Year 2002

ISBN 974-17-0959-5

Thesis Title	SEPARATION OF ISOFLAVONES FROM SOYBEAN FLAKE EXTRACTS BY HIGH PERFORMANCE LIQUID CHROMATOGRAPHY
By	Nattada Junghuttakarnsatit
Field of study	Chemical Engineering
Thesis Advisor	Dr. Muenduen Phisalaphong
Thesis Co-advisor	Dr. Terasut Sookkumnerd

Accepted by the Faculty of Engineering, Chulalongkorn University in Partial Fulfillment of Requirements for the Master's Degree

..... Dean of Faculty of Engineering
(Professor Somsak Panyakeow, D.Eng.)

THESIS COMMITTEE

..... Chairman
(Associate Professor Tharathon Mongkhonsi, Ph.D.)
..... Thesis Advisor
(Muenduen Phisalaphong, Ph.D.)
..... Thesis Co-advisor
(Terasut Sookkumnerd, Ph.D.)
..... Member
(Assistant Professor Prasert Pavasant, Ph.D.)
..... Member
(Assistant Professor Seeroong Prichanont, Ph.D.)

ณัฐดา จูงหัตถการสาธิต: การแยกไอโซฟลาโวนจากสารสกัดจากกากถั่วเหลืองโดยโครมาโตกราฟีแบบของเหลวสมรรถนะสูง. (SEPARATION OF ISOFLAVONES FROM SOYBEAN FLAKE EXTRACTS BY HIGH PERFORMANCE LIQUID CHROMATOGRAPHY) อาจารย์ที่ปรึกษาวิทยานิพนธ์: อาจารย์ ดร. เหมือนเดือน พิศาลพงศ์, อาจารย์ที่ปรึกษาร่วม: อาจารย์ ดร. ธีระสุต สุขกำเนิด, 89 หน้า. ISBN 974-17-0959-5

งานวิจัยนี้มีจุดมุ่งหมายเพื่อพัฒนาแบบจำลองสำหรับการแยกสารไอโซฟลาโวนจากสารสกัดจากกากถั่วเหลืองในระบบโครมาโตกราฟีแบบของเหลวสมรรถนะสูง และ เพื่อได้รับข้อมูลที่เป็นประโยชน์ในการแยกไอโซฟลาโวนในระบบโครมาโตกราฟี จากการทดลองพบว่าเฟสของไหลที่เหมาะสมที่สุดในการแยกไอโซฟลาโวนจากสารสกัดจากกากถั่วเหลือง คือ สารละลายเมทานอล 33% ในน้ำ ในการสร้างแบบจำลองสำหรับการแยกสารไอโซฟลาโวนนั้นต้องอาศัยสมการการดุลมวลสารและสมการการดูดซับ โดยสมการการดูดซับที่ใช้เป็นกรณีไอโซเทอมแบบเชิงเส้น ค่าพารามิเตอร์ต่างๆที่ต้องใช้ในแบบจำลอง ได้แก่ ความพรุนของเฟสหยุดนิ่ง ความพรุนของเบด การกระจายตัวในแนวแกน ค่าคงที่ของการดูดซับ และ ค่าคงที่ของการถ่ายโอนมวลสารหาได้จากการทดลองและสมการความสัมพันธ์ต่างๆ พบว่าแบบจำลองที่ไม่รวมเทอมการกระจายตัวในแนวแกนสามารถทำนายได้ดีเช่นเดียวกับกรณีที่รวมเทอมนี้ แต่ใช้เวลาในการคำนวณน้อยกว่า 8 ถึง 9 เท่า และแบบจำลองนี้ยังสามารถทำนายในกรณีที่ความเข้มข้นของไอโซฟลาโวนที่ฉีดเปลี่ยนแปลง และ ในกรณีที่ความเร็วของเฟสเคลื่อนที่เปลี่ยนแปลงได้เป็นอย่างดี นอกจากนี้งานวิจัยยังหาความสัมพันธ์ของค่าคงที่ของการดูดซับกับค่าความเข้มข้นของเมทานอลในน้ำของเฟสเคลื่อนที่ในช่วง 25% ถึง 40% ปริมาตรต่อปริมาตร จากการทดลอง พบว่า ความสัมพันธ์ที่ได้มีลักษณะเป็นเชิงเส้น

ภาควิชา วิศวกรรมเคมี	ลายมือชื่อนิสิต.....
สาขาวิชา วิศวกรรมเคมี	ลายมือชื่ออาจารย์ที่ปรึกษา.....
ปีการศึกษา 2545	ลายมือชื่ออาจารย์ที่ปรึกษาร่วม.....

##4370287721 : MAJOR CHEMICAL ENGINEERING
KEYWORD: ISOFLAVONES / HIGH PERFORMANCE LIQUID CHROMATOGRAPHY / SIMULATION / PARAMETER ESTIMATION

NATTADA JUNGHUTTAKARNSATIT: SEPARATION OF ISOFLAVONES FROM SOYBEAN FLAKE EXTRACTS BY HIGH PERFORMANCE LIQUID CHROMATOGRAHY. THESIS ADVISOR: MUENDUEN PHISALAPHONG, Ph.D. THESIS COADVISOR: TERASUT SOOKKUMNERD, Ph.D., 89 PP. ISBN 974-17-0959-5

The simulation and the useful information for the separation of isoflavones (Daidzin and Genistin) in soybean flake extracts by High Performance Liquid Chromatography (HPLC) were obtained. In this study, the most suitable mobile phase for the separation of isoflavones from soybean flake extracts was 33% methanol aqueous solution. For setting up the simulation, the mass balance and linear adsorption isotherm were used. The modeling parameters in the simulation estimated from the experiment and the correlation were internal porosity, external porosity, axial dispersion coefficient, adsorption equilibrium constant, and mass transfer coefficient. It was found that the simulation without the axial dispersion term was the same as the simulation with this term but required time eight to nine-fold less. The simulation could predict the separation in HPLC system well when the injected concentration and the velocity of mobile phase were changed. Furthermore, the relationship between the adsorption equilibrium constant and the concentration of methanol in the mobile phase in the range of 25% to 40% vol/vol aqueous solution was found from the experiment to be linear.

Department	Chemical Engineering	Student's signature……
Field of Study	Chemical Engineering	Advisor's signature……...
Academic year	2002	Co-Advisor's signature…….

ACKNOWLEDGEMENTS

This thesis had not been achieved utterly, if I would not have acquired invaluable suggestion, kind support, and tireless guidance from my advisor, Dr. Muenduen Phisalaphong. I would like to express my sincere gratitude to her for priceless things she has done for me. To my co-advisor, Dr. Terasut Sookkumnerd, I am grateful to him for his excellent supervision and powerful superintendence. His advice made the work go smoothly. I am appreciated to Associate Professor Dr. Tharathon Mongkhonsi, Chairman of the committee, Assistant Professor Dr. Prasert Pavasant, and Assistant Professor Dr. Seeroong Prichanont, members of thesis committee, for many valuable comments.

For two a half years I have studied Master degree of Chemical Engineering in Biochemical Engineering research group, I have got a great life experience. Every member in the research group taking care of me with warmth is thankworthy for their friendly support. Particularly Porntip Wongsuchoto, who is both of my respectful senior and reliable friend, always listens all of my problems and cheers me up when I fail, thank you indeed. Special thanks to members of Safety and Environmental research group, who filled me a part of my life and worked with me at night.

Beyond everything, the extremely absolutely priceless things that I have are my parents' support and understanding. I would like to express my utmost gratitude to them. My sister who is my true friend always cheers me up and gives me inspiration. Thank you indeed.

CONTENTS

PAGE

CONTENTS(Cont.)

PAGE

CONTENTS(Cont.)

PAGE

CONTENTS(Cont.)

PAGE

LIST OF TABLES

TABLE **PAGE**

LIST OF FIGURES

FIGURES **PAGE**

LIST OF FIGURES (Cont.)

FIGURES **PAGE**

LIST OF FIGURES (Cont.)

FIGURES **PAGE**

NOMENCLATURE

a_p External surface of the adsorbent pellet [m^2/m^3]

A Crossectional area of HPLC column [m^2]

AU Absorbance unit [AU]

A_t Crossectional area of tube connecting HPLC column with autosample injector and UV detector [m^2]

C Concentration in the fluid phase [$kmol/m^3$]

C_j Concentration of daidzin or genistin in the soybean flake extracts sample [$kmol/m^3$]

C_p Concentration in the macropore [$kmol/m^3$]

d_p Equivalent particle diameter [m]

D_L Axial dispersion coefficient [m^2/s]

D_{mi} Molecular diffusion coefficient [m^2/s]

k Overall mass transport coefficient [m/s]

K Equilibrium constant

ℓ Light path length [m]

L Column length [m]

L_d Length of tube connecting HPLC column and autosample injector and UV detector [m]

$M.W.$ Molecular weight [kg/kmol]

NC Total number of components

Pe Peclet's number = $\frac{u_r d_p}{D_L}$

q Dimensionless adsorbed phase concentration

Q Volumetric flow rate [m^3/s]

Re Reynold's number = $\frac{\rho u d_p}{\eta}$

St Stanton's number = $\frac{k a_p L}{u_r}$

NOMENCLATURE(Cont.)

t	Time [s]
t_{de}	Dead time [s]
t_{max}	Residence time of peak maximum [s]
t_p	Time during the constant concentration c_f is fed into column [s]
u	Interstitial velocity [m/s]
V_j	Injection volume [m^3]
V_p	Pore volume [m^3]
V_{total}	Column volume [m^3]
x	Dimensionless axial coordinate
y	Dimensionless concentration in fluid phase
y_p	Dimensionless concentration in the macropore
z	Axial coordinate [m]

Greek letters

ε	Extinction coefficient [AU/m-g/l]
ε_e , ε_p	External, internal void fraction
Γ	Adsorbed phase concentration [kmol/m^3]
η	Viscosity [kmol/m-s]
ρ	Fluid molar density [kg/m^3]
ρ_p	Particle density [kg/m^3]
τ	Dimensionless time
τ_p	Dimensionless time during the constant dimensionless concentration y_f is fed into column
ξ	Dimensionless fluid interstitial velocity = $\frac{u}{u_r}$

NOMENCLATURE(Cont.)

Subscripts

d	daidzin
f	Inlet value
g	genistin
i	Index component
m	methanol
r	Reference condition
s	Packing

Superscript

0	Initial value

CHAPTER 1
Introduction

1.1 General Ideas

Soybean and its processed products have been used as food in the Orient for centuries. They are known to contain a number of components, which may have beneficial biological effects in the diet. Soybean is a particularly abundant source of phytoestrogens of the isoflavone class. There is a significant carry over of soy phytoestrogens into its processed products (Murphy, 1982; Wang et al., 1990; Coward et al., 1993; Wang and Murphy, 1994, 1996; Fukutake et al., 1996; Hui et al., 2001; Hutabarat et al., 2001).

Isoflavone is one of phytoestrogen compounds, which have the same effects as estrogen hormone in human body. The major isoflavones in soybean are phytoestrogens, genistein and daidzein, and their glucoside derivatives, genistin and daidzin. Genistein and daidzein have attracted a great deal of recent interests owing to their potential property with low incidence rates of hormonally dependent and independent cancers such as bowel cancers, breast cancers and prostate cancers (Setchell et al., 1981; Setchell et al., 1984; Messina and Barnes, 1991; Peterson and Barnes, 1991). Soy food has been associated with a lower risk of cardiovascular diseases (Anderson et al., 1995). Isoflavones might directly inhibit bone resorption (Arjmandi et al., 1996) and might be the factor responsible for the cholesterol-lowering property of some soy foods (Anthony et al., 1996).

In soybean and food derived from soy, isoflavones were found ranging from 0.1 to 5 mg/g of dry weight (Coward et al., 1993). In general, isoflavones have been extracted from soy with a hot aqueous polar solvent such as methanol or acetonitrile (Murphy, 1981; Eldridge, 1982; Barnes et al., 1994; Hutabarat et al., 1998; Choi and Row, 2000). High performance liquid chromatography (HPLC) has been generally used for analysis of isoflavones. It could separate isoflavones quite well (Carlson and

Dolphin, 1978, 1980; West et al., 1978; Murphy, 1981; Eldridge, 1982; Farmakalidis and Murphy, 1985; Wang et al, 1990; Barnes et al., 1994; Song, 1998; Hutabarat et al., 1998; Choi and Row, 2000). Therefore, HPLC can be a good choice for separation and purification of isoflavones in soybean extracts.

Chromatographic methods have been developed to detect and isolate various components particularly in pharmaceutical industries over the past two decades. The general basic for the separation based on the difference of mass transfer of each component to the surface and into the bulk of a solid or liquid. HPLC appears to be a very powerful purification technique, however, it is often considered as a very expensive technique, not really applicable on a large scale. This is indeed the case when the operating conditions are not optimized. By selecting the chromatographic parameters carefully, purification costs can be reduced to a level that makes HPLC economically competitive with other purification technique.

Simulations of HPLC separation have been proposed for the analysis and optimization. Several researchers (Yu and Wang, 1989; Sereno et al., 1991, 1992; Berninger et al., 1991; Ma and Guichon, 1991; Kaczmarki, 1996) reported the simulation of non-linear multicomponent chromatography by using finite element and finite difference. Such mathematical model was based on mass balance and adsorption equilibrium. The model was time-dependent and could be used to predict the transient behavior of the system.

In this study, pulse response experiments and mathematical model for the analysis elution of isoflavone separation from soybean flake extracts by reverse-phase HPLC are performed. The results will provide understanding of mass transfer characteristic for isoflavone separation in HPLC system and may be used for the design of HPLC separation process.

1.2 Objectives

1. To develop a suitable simulation model for the separation of isoflavones in HPLC system.
2. To obtain useful information for preparative separation of isoflavones from soybean flake extracts by HPLC.

1.3 Scopes of the Work

1. Separation of isoflavones is carried out by HPLC system equipped with a UV-detector at 262 nm using a HiQsil C_{18} reverse-phase (250 × 4.6 mm) column.
2. Acetonitrile-water, ethanol-water, and methanol-water are applied to determine the suitable mobile phase.
3. The values of the unknown modeling parameters have to be determined. BET and Pore Sizer are used for the estimation of internal porosity. Axial dispersion is calculated from semiempirical relationship for packed-beds. Adsorption equilibrium can be obtained from the first moment analysis. Blue dextran is used as pulse tracer for the estimation of external porosity.
4. The superficial velocity of mobile phase in the HPLC column in this work ranges from 8.023×10^{-4} to 1.404×10^{-3} $m \cdot s^{-1}$ (limited by the maximum pressure allowance (less than 4000 psi) for the HPLC column.
5. Daidzin and genistin are the only two components in the soybean flake extracts to be simulated in this work.
6. The concentration of daidzin and genistin used in this work is between 0.009 to 0.072 mg/ml and 0.004 to 0.016 mg/ml, respectively, for which the adsorption isotherm is found linear.

CHAPTER 2

Backgrounds and Literature Reviews

2.1 Backgrounds

2.1.1 Isoflavones

Isoflavone is one of phytoestrogens, which are the natural product from plant. Clinical effects of phytoestrogens are like steroidal estrogen hormone such as oestradiol in women because phytoestogens are structurally similar to mammalian oestradiol (Setchell and Adlercrueutz, 1988). Accordingly, they can bind to estrogen receptors, albeit at comparatively low levels (Shutt and Cox, 1972; Miksicek, 1995) as shown in Figure 2.1.1. *In vitro* studies have established that phytoestrogens are weakly estrogenic. They have affinity to receptors about 10 to 1000 times lower than oestradiol. However, although these weak estrogens bind to the estrogen-receptor complex, they fail to stimulate a full estrogenic response of replenishment of estrogen receptor (Tang and Adams, 1980). This raises the possibility that they may be protective in hormone-related disease, such as breast cancer and prostate cancer (Setchell et al., 1981; Peterson and Barnes, 1991).

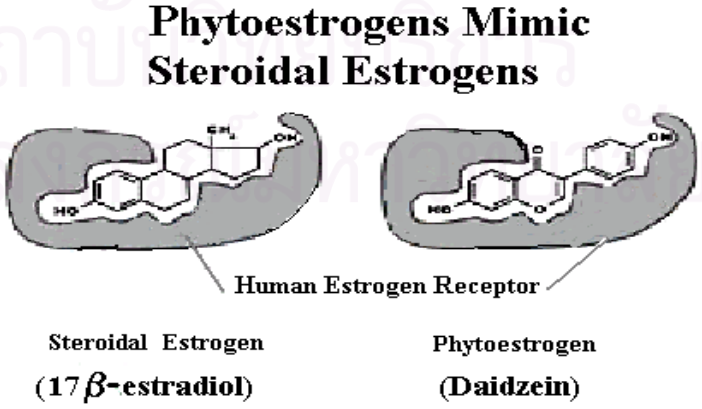

Figure 2.1.1. The structural similarity of mammalian steroidal estrogen (17β-estradiol) and phytoestrogen (daidzein)

Phytoestrogen are commonly found in 5 groups; flavones, flavonols, flavonones, isoflavones and lignans. Isoflavones can be found in soybean or soybean products.

2.1.2 Isoflavones in Soybean

In soybean, isoflavones are conjugated with glucose (to form glucosides); the major glucosides are daidzin, genistin and glycitin. These conjugated forms are not active oestrogenically (Miksicek, 1995). Bacteria in the rumen are known to deconjugate the glycosides to aglycones, daidzein, genistein and glycitein. The structure of these compounds is shown in Figure 2.1.2.

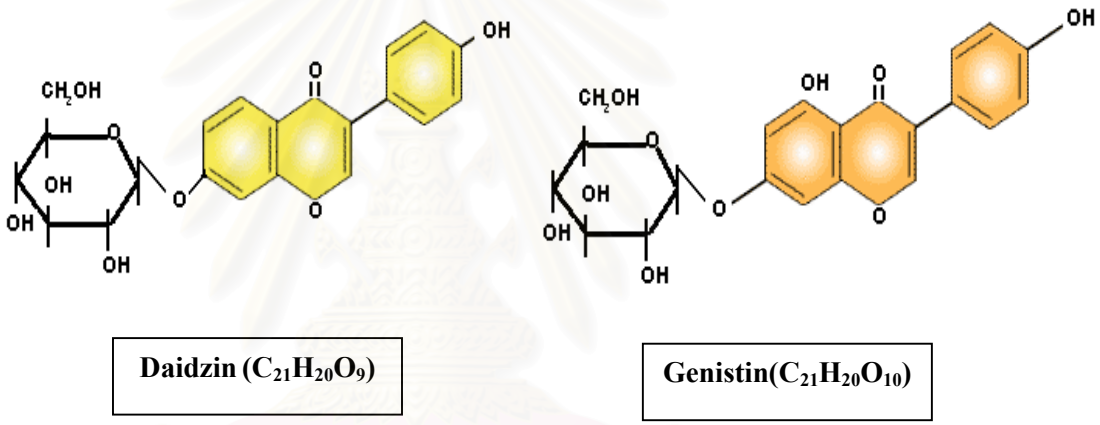

(a)

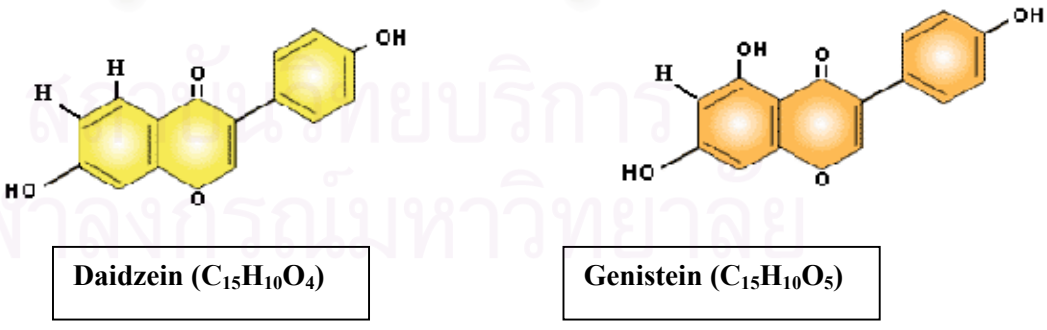

(b)

Figure 2.1.2 The structure of isoflavones: (a) glucosides (daidzin and genistin); (b) isoflavone aglucones (daidzein and genistein).

In soybean, 3 aglycones and 9 glucosides are found. The structure of isoflavones and conjugated isoflavones is shown in Figure 2.1.3.

Aglycones

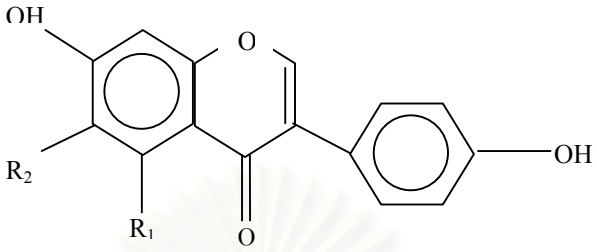

R1	R2	Compound
H	H	Daidzein
OH	H	Genistein
H	OCH_3	Glycitein

Glucosides

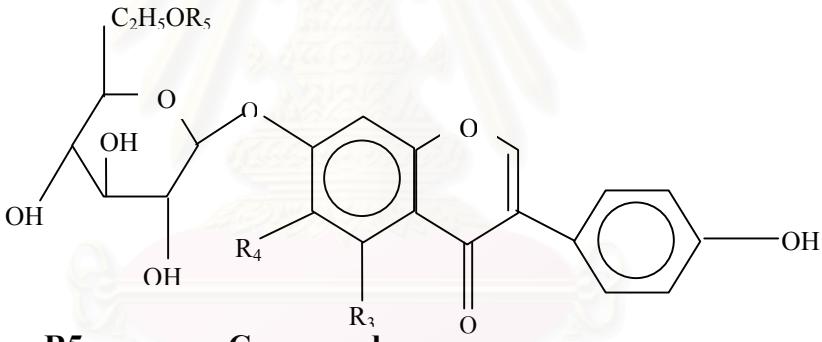

R3	R4	R5	Compound
H	H	H	Daidzin
OH	H	H	Genistin
H	OCH_3	H	Glycitin
H	H	$COCH_3$	Acetyldaidzin
OH	H	$COCH_3$	Acetylgenistin
H	OCH_3	$COCH_3$	Acetylglycitin
H	H	$COCH_2COOH$	Malonyldaidzin
OH	H	$COCH_2COOH$	Malonylgenistin
H	OCH_3	$COCH_2COOH$	Malonylglycitin

Figure 2.1.3. The structure of 12 isoflavones; 3 aglucosides and 9 glucoside isoflavones are found in soybean extracts.

Isoflavone concentrations in soyfoods and soybeans can vary and are dependent on the soybean and processing conditions used to produce a particular food product. The distribution of different forms of isoflavones represents a history of the processing of these foods. Heat processing, enzymatic hydrolysis, and fermentation can significantly alter the isomeric distribution of isoflavones (Wang and Murphy, 1994). The content of isoflavones in soybean and soybean product is shown in Table 2.1.

Table 2.1 shows the content of isoflavones in soybean product (Wang & Murphy, 1994)

Product	Daidzein (mg/100g)	Genistein (mg/100g)	Glycetein (mg/100g)	Total (mg/100g)
Roasted soybeans	56.3	86.9	19.3	162.5
Textured vegetable protein	47.3	70.7	20.2	138.2
Green soybean	54.6	72.9	7.9	135.4
Soyflour	22.6	81.0	8.8	112.4
Tempeh	27.3	32.0	3.2	62.5
Tofu	14.6	16.2	2.9	33.7
Tofu yogurt	5.7	9.4	1.2	16.4
Soy hot dog	3.4	8.2	3.4	15.0
Soy noodle (dry)	0.9	3.7	3.9	8.5

2.1.3 High Performance Liquid Chromatography

High Performance Liquid Chromatography (HPLC) is a popular method of analysis because it is easy to learn and use and is not limited by the volatility or stability of the sample compound. Modern HPLC has many applications including separation, identification, purification, and quantification of various compounds. HPLC is widely considered to be a technique mainly for biotechnological, biomedical, and biochemical research as well as for the pharmaceutical industry. Currently HPLC is used in a variety of fields including cosmetics, food, and environmental industries.

HPLC involves injecting a pulse of solute into one end of the column, and then following the pulse with solvent. Eventually, the pulse comes out the other end of the column. The pulse enters as a narrow, concentrated peak, but it exits dispersed and diluted by the additional solvent. In HPLC, the goal is to purify the product even when it is diluted.

Pulses of different solutes all leave the bed diluted, but they leave at different times, as suggested schematically in Figure 2.1.4. Three solutes, shown as circles, triangles, and squares are injected as a pulse into one end of a column, shown as the horizontal lines. Solvent flows from left to right in the column, displacing the original (shaded) contents. The solute shown as squares is not adsorbed much, so it is swept along quickly; the solute shown as circles is most strongly adsorbed, so it is most retarded. The squares reach the end of the column first, and so are eluted first as shown in the graph at the bottom of the figure. The triangles and circles exit later. This difference in elution is the source of the purification. The price of this purification is dilution with mobile phase.

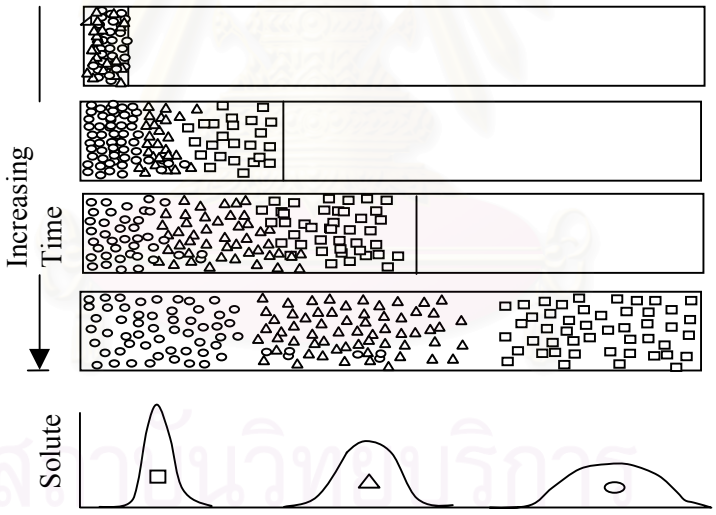

Figure 2.1.4. Concentrations in elution chromatography. Three solutes, shown schematically as circles, triangles, and squares are injected into one end of a packed bed. When solvent flows through the bed from left to right, the three solutes move at different rates because of different adsorption. They exit at different times, and hence are separated.

Main equipment of HPLC system is composed of pump, injector, guard column, HPLC column, and detector. The connection of each HPLC apparatus is shown in Figure 2.1.5.

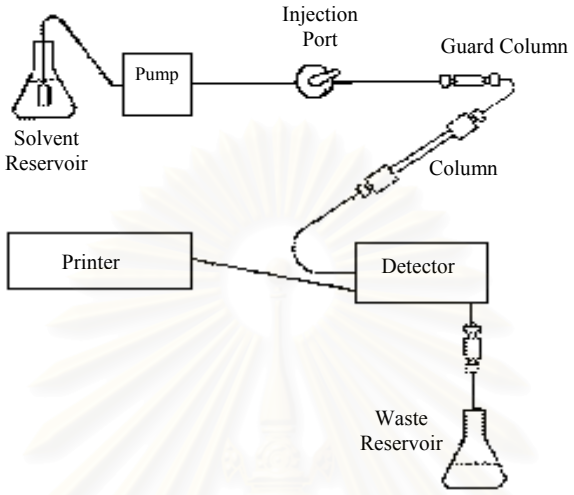

Figure 2.1.5. Schematic representation of the connection of HPLC apparatus

2.1.3.1 Mobile Phase of HPLC

The mobile phase in HPLC refers to the solvent being continuously applied to a column, or stationary phase. The mobile phase acts as a carrier for sample solution. The sample solution is injected into the mobile phase of an assay through an injector port. As the sample solution flows through the column with the mobile phase, the components of that solution migrate according to the non-covalent interactions of the compound with the stationary phase of the column. The chemical interactions of the mobile phase and the sample with the stationary phase determine the degree of migration and separation of components contained in the sample. The mobile phase can be altered in order to manipulate the interactions of the sample and the stationary phase. There are several types of mobile phases, these include: Isocratic, gradient, and polytyptic.

In isocratic elution compounds are eluted using constant mobile phase composition. All compounds begin migration through the column at onset. However, each migrates at a different rate, resulting in faster or slower elution rate. This type of

elution is both simple and inexpensive, but resolution of some compounds is questionable and elution may not be obtained in a reasonable amount of time.

In gradient elution, different compounds are eluted by increasing the strength of the organic solvent. The sample is injected while a weaker mobile phase is being applied to the system. The strength of the mobile phase is later increased in increments by raising the organic solvent fraction, which subsequently results in elution of retained components. This is usually done in a stepwise or linear fashion. Compared with isocratic elution, resolution and separation are improved.

2.1.3.2 Stationary Phase

The stationary phase in HPLC refers to the solid support contained within the column over which the mobile phase continuously flows. The sample solution is injected into the mobile phase of the assay through the injector port. As the sample solution flows with the mobile phase through the stationary phase, the components of that solution will migrate according to the non-covalent interactions of the compounds with the stationary phase. The chemical interaction of the stationary phase and the sample with the mobile phase, determines the degree of migration and separation of the components contained in the sample. Columns containing various types of stationary phases are commercially available. Some of the more common stationary phases include: Liquid-Liquid, Liquid-Solid (Adsorption), Size Exclusion, Normal Phase, Reverse Phase, Ion Exchange, and Affinity.

Reverse Phase operates on the basis of hydrophilicity and lipophilicity. The stationary phase consists of silica based packings with n-alkyl chains covalently bound. For example, C-8 signifies an octyl chain and C-18 an octadecyl ligand in the matrix. The more hydrophobic the matrix on each ligand, the greater is the tendancy of the column to retain hydrophobic moieties. Thus hydrophilic compounds elute more quickly than do hydrophobic compounds.

2.2 Literature Reviews

2.2.1 Isoflavones Benefits

Soybeans contain a number of components, which may have beneficial biological effects in the diet. The soybean is a particularly abundant source of phytoestrogens of the isoflavone class. Interest in isoflavones has received increasing attention in recent years from health care providers, biomedical researchers and the general people because of its potential role in the prevention and treatment of a number of diseases. Dran et al. (1979) determined estrogenic activity of sixteen samples of soy meal in mouse uterine weight bioassay and all samples were found to have estrogenic activity. Pratt and Birac (1979) studied about antioxidant in soybean, defatted soy flour, soy protein concentrates, and soy isolates. Soybean and soy products possess appreciable antioxidant activity.

Isoflavones had an ability to play a role in the prevention of certain cancers. Several groups of researchers (Setchell et al., 1981; Setchell et al., 1984; Messina and Barnes, 1991; Peterson and Barnes, 1991) found that isoflavones had potential property with low incidence rate of hormonally dependent and independent cancers such as breast cancer, prostate cancer, bowel cancer. They suggested that genistein was the agent in soy, which accounted for the apparent association between increases in soy food consumption and reduction of cancer risk. It was a potent inhibitor of the growth of cell lines. Messina and Barnes (1991) observed Oriental women, who had low incidence rates of breast cancer, consumed larger amounts of soy products than did most American women. However, although fertility and reproduction in animals were adversely affected by ingestion of plant isoflavones, the amount of isoflavones in soy products consumed by Oriental women did not appear to affect their reproductive capacity. In addition, isoflavones were partly responsible for the cholesterol-lowering effect in animals. Anthony et al. (1996) found that soybean isoflavones had favorable effects on plasma lipid and lipoprotein concentrations, specifically by significantly reducing cholesterol concentrations in both males and females monkeys. The isoflavones in soy protein improved cardiovascular disease risk factors without apparent effects on the reproductive system of monkeys.

Furthermore, isoflavones had a role of treatment osteoporosis. Arjmandi et al. (1996) found that one of three groups of rats, which was fed with soybean protein instead of casein, was not observed lower bone densities like other groups. Their findings suggested that dietary soybean protein was effective in preventing bone loss due to ovarian hormone deficiency.

2.2.2 Separation of Isoflavones from Soybean Materials by High Performance Liquid Chromatography

High performance liquid chromatography (HPLC) is the method most often used to separate and quantitate phytoestogens in plants and food products. In 1978, West et al. developed an isocratic HPLC method to separate 4′,6,7-trihydroxyisoflavone and genistein. Separations were carried out with a mobile phase of water-acetonitrile 4: 1 at a rate 1.8 ml/min. Further, Murphy (1981) used a non-linear methanol-water gradient HPLC techniques to separate isoflavones in soybean flake extracts. Eldridge (1982) used a methanol-water gradient HPLC to separate isoflavones glucosides and aglycones in hexane-defatted soybean meal. Eldridge found that glucosides eluted first and were followed by isoflavone aglycones. The eight peaks were separated, they are daidzin, glycitein-7-β-O-glucoside, genistin, daidzein, glycitein, genistein, coumesterol and *n*-butyrophenone. The amounts (mg/100g) of isoflavones in hexane-defatted soybean meal have been found to be: daidzin, 62; glycitein-7-β-O-glucoside, 18; genistin, 127; daidzein, 48; glycitein, trace; genistein, 40. Wang et al. (1990) determined isoflavones in soybean and its processed products by isocratic HPLC without defatting and cleanup of the samples prior to assay. Coward et al. (1993) used a gradient acetonitrile-water HPLC method to separate isoflavones β-glucoside conjugates and aglycones from various foods derived from soybeans of both American and Asian origin. The gradient HPLC method was also used by Barnes et al. (1994); Wang and Murphy (1996) for analysis isoflavones in soy foods. Gugger et al. (1997) separated isoflavones by using ultrafiltration membrane and purified by crystallization unit. Nearly 50% of isoflavones could not pass through the ultrafiltration unit. Song et al. (1998) analyzed soy isoflavone contents of soy foods by using a gradient acetonitrile-water-acid HPLC. The 12 isoflavone isomers was separated-3 aglycones (daidzein, genistein, and glycitein) and 9 glucosides (daidzin, genistin, glycitin, acetyldaidzin, acetylgenistin,

acetylglycitin, malonyldaidzin, malonylgenistin, and malonylglycitin). The resolution was quite well established. Hutabarat et al. (1998) developed an isocratic HPLC method for the analysis of daidzein, genistein, and biochanin A in soybean. Recently, Choi and Row (2000) used preparative column (1" × 25 cm) to separate isoflavones from soybean. The mobile phases were the ternary system of water, acetonitrile, and acetic acid at volumetric flow rate of 18 ml/min and 2 ml of samples were injected. Some isoflavones (daidzein, glycitin, daidzin, and glycitein) could be purely collected.

2.2.3 Simulation of High Performance Liquid Chromatography

Finite difference method was used to simulate the elution profiles of High Performance Liquid Chromatography in many researches. Experimental studies have demonstrated excellent agreement between the individual band profiles observed and the predictions made by these calculations (Rouchon et al., 1987; Czok and Guiochon, 1990a, b; Ma and Guiochon, 1991; Kaczmarski, 1997). These authors also showed that the effect caused by the dispersion term in a material balance equation could be the same as that caused by numerical diffusion generated in the finite difference method if the dispersion term was neglected but the space and time increment of the finite difference method are properly chosen.

Kaczmarski (1997) solved nonlinear chromatography column model by using two numerical procedures. First solution technique was based on the method of lines, in which the space variables were discretized using the orthogonal collocation method on moving finite element. This model included axial dispersion in the external fluid phase. Second solution technique was a very fast finite difference method in which the axial dispersion term was ignored. This model was presented less accurate but faster results than an orthogonal collocation method.

Park et al. (2000) simulated of separation taxol from yew tree by normal phase HPLC with finite difference method. The axial dispersion term was not included in the model. The agreement between the experimental data and the simulation results was relatively good.

CHAPTER 3

Materials and Methods

3.1 Experimental Apparatus and Materials

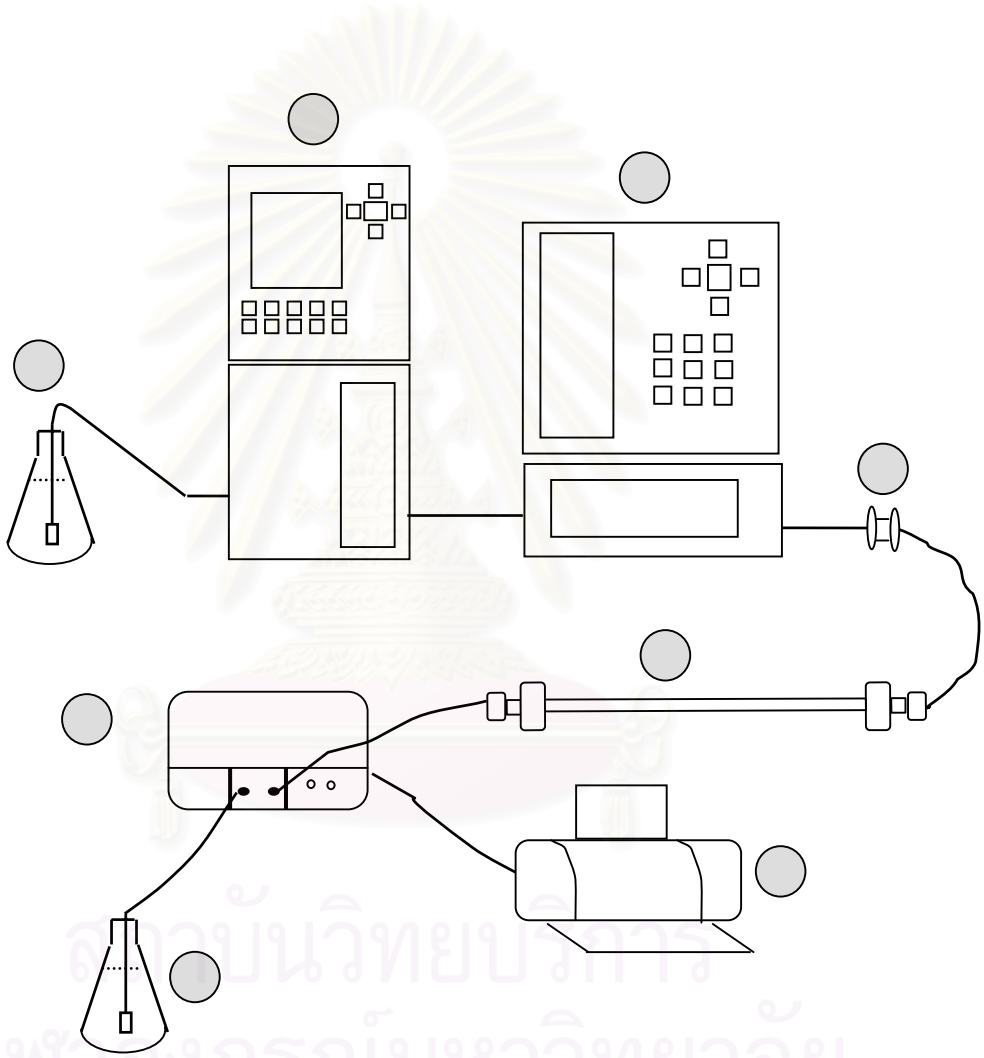

Figure 3.1 Schematic diagram of the High Performance Liquid Chromatography system. 1.Solvent Reservoir, 2.Pump, 3.Autosample Injector, 4.Guard Column, 5.HPLC Column, 6.Detector, 7.Waste Reservoir, 8.Printer.

A schematic diagram of the High Performance Liquid Chromatography (HPLC) system is shown in Figure 3.1. The following equipment was used: a Waters model 600 pump; a Waters model 717 autosample injector; a Waters model 996 UV-photodiode array detector, and a KYA Tech Corporation HiQ sil C_{18} reversed-phase column (4.6 mm id., 250 mm, SS). The HPLC column was packed with spherical packing material with 100 Å in pore size diameter and 5 μm in packing diameter. The column was protected by a Waters μBond apak^{TM} C_{18} guard column and was maintained at ambient temperature (30°C) and constant pressure during the operation. The methanol 33% in water in isocratic mode was used as the mobile phase and the absorption was measured at 262 nm. Prepared samples at different concentration of daidzin and genistin was auto-injected at 10 μl of injection volume into the column at different volumetric flow rate of mobile phase (varied from 0.8 to 1.4 ml/min). The concentration of daidzin and genistin ranged from 0.009 to 0.072 mg/ml and 0.004 to 0.016 mg/ml, respectively. UV spectra were recorded, and area responses were integrated by Waters Millenium Software Program. Experimental conditions and the characteristic of the experimental equipment are summarized in Table 3.1.

HPLC grade water, methanol, and ethanol purchased from Labscan Asia were used without further purification. The isoflavones standards, genistin and daidzin were purchased from Fluka Chemika Co. Blue dextran used as a pulse tracer was purchased from Sigma Chemical Co. C_{18} packing was purchased from Sittiporn Associate, Thailand.

Table 3.1 Experimental conditions and the characteristic of the experimental apparatus

Model of High Performance Liquid Chromatography system	Waters 600, 717, 996
Type of detector	UV
Type of HPLC column	C_{18}-reversed phase
Inner diameter of HPLC column	4.6 mm
Length of HPLC column	250 mm
Pore size diameter of packing material	100 Å
Diameter of packing material	5 μm
Guard column	Waters μBond apak™
Temperature	Ambient (30°C) and constant
Pressure	Constant
Type of mobile phase	Methanol 33% in water
Absoption wave length	262 nm
Volume of injection	10 μl
Flow rate of mobile phase	0.8 – 1.4 ml/min
Concentration of daidzin	0.009 – 0.072 mg/ml
Concentration of genistin	0.004 – 0.016 mg/ml

3.2 Experimental Methods

3.2.1 Preparation and Analysis of Soybean Flake Extract Sample

1. Filtrate from pre-purification of soybean flake extracts by microfiltration unit was used as the samples for this study. The methods for the extraction and the pre-purification are cited in Appendix B.
2. Prepared soybean flake extract was kept at -4°C as the stock solution and was then diluted to the assigned concentration with 75% ethanol solution.
3. The samples were filtrated through 0.2 μm PTFE microfilter (KYA Tech Corporation) and collected into 1 ml vials for HPLC analysis (as described in section 3.1). The analyzed data was qualified and quantified against the daidzin and genistin standards.

3.2.2 HPLC Preparation

In this study, all experiments using the HPLC system are subject to the preparation described in this section.

1. Degas mobile phase in ultrasonic bath for 30 minutes.
2. Degas the HPLC system, and stabilize the UV detector by means of flowing 100% methanol at 1 ml/min for 2 hours.
3. Equilibrate the HPLC column by flowing a decided mobile phase at a flow rate of 1 ml/min for 30 min.
4. Set the UV detector at 262 nm.
5. Set pump at a decided flow rate of the HPLC pump.
6. Check baseline of the HPLC system; the baseline must become constant before injecting sample.

3.2.3 Selection of Suitable Mobile Phase

1. Review safety data sheet of solvents applied for the mobile phase of isoflavone separation i.e., acetonitrile, methanol, and ethanol.
2. Perform pulse response experiments with different mobile phase (acetonitrile-water, ethanol-water and methanol-water) at volumetric flow rate 1 ml/min.
3. Analyze the obtained data and select the mobile phase for the isoflavone separation.
4. Adjust the concentration of mobile phase to determine the optimum concentration that peaks of daidzin and genistin can be separated, base on separation performance and minimum run time.

CHAPTER 4

Mathematical Model

4.1 Derivation of Mathematical Model for High Performance Liquid Chromatography

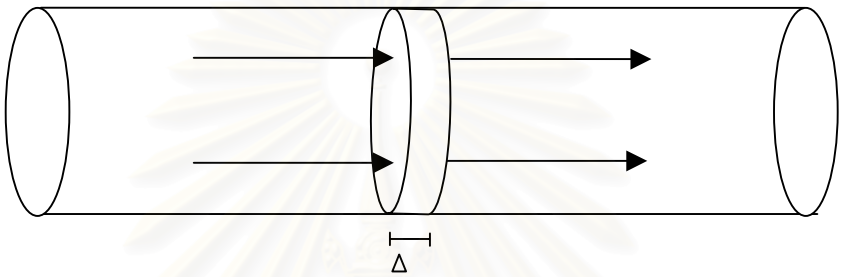

Figure 4.1. Mass transfer in the packed-circular tube

Mathematical model for liquid chromatography is based on material balance and adsorption equilibrium. The assumptions for the derivation of the model are summarized here.

1. One-dimensional column in the direction of the flow, with constant cross-sectional area.
2. Axially dispersed plug flow of the fluid phase.
3. Constant-velocity of the fluid phase.
4. Constant void fraction along the bed.
5. Linear driving force model for mass transport.
6. Spherical solid particles with constant porosities.
7. Constant pressure.
8. Constant temperature.

Material balance of i^{th} component in mobile fluid phase

From material conservative law:

Accumulation in liquid and in packing =	*Solute dispersion in-out* +	*Solute convection in-out*

Accumulation in liquid : $\varepsilon_e A\Delta z \frac{\partial \rho_i}{\partial t}$ (4.1.1)

Accumulation in packing : $(1-\varepsilon_e) A\Delta z \frac{\partial \rho_s}{\partial t}$ (4.1.2)

Solute dispersion in-out : $-\varepsilon_e A D_L \frac{\partial \rho_i}{\partial z}\Big|_Z - \left(-\varepsilon_e A D_L \frac{\partial \rho_i}{\partial z}\Big|_{Z+\Delta Z}\right)$

$$= \varepsilon_e A D_L \frac{\partial \rho_i}{\partial z}\Big|_{Z+\Delta Z} - \varepsilon_e A D_L \frac{\partial \rho_i}{\partial z}\Big|_Z \quad (4.1.3)$$

Solute convection in-out : $\varepsilon_e A u \rho_i \Big|_Z - \varepsilon_e A u \rho_i \Big|_{Z+\Delta Z}$

$$= -\left(\varepsilon_e A u \rho_i \Big|_{Z+\Delta Z} - \varepsilon_e A u \rho_i \Big|_Z\right) \quad (4.1.4)$$

We now add up the contributions to the material balance;

$$\varepsilon_e A\Delta z \frac{\partial \rho_i}{\partial t} + (1-\varepsilon_e) A\Delta z \frac{\partial \rho_s}{\partial t} = \varepsilon_e A D_L \frac{\partial \rho_i}{\partial z}\Big|_{Z+\Delta Z} - \varepsilon_e A D_L \frac{\partial \rho_i}{\partial z}\Big|_Z - \left(\varepsilon_e A u \rho_i \Big|_{Z+\Delta Z} - \varepsilon_e A u \rho_i \Big|_Z\right) \quad (4.1.5)$$

Dividing Eq. 4.1.5 with $A\Delta z$ gives:

$$\varepsilon_e \frac{\partial \rho_i}{\partial t} + (1-\varepsilon_e) \frac{\partial \rho_s}{\partial t} = \left(\varepsilon_e D_L \frac{\partial \rho_i}{\partial z}\Big|_{Z+\Delta Z} - \varepsilon_e D_L \frac{\partial \rho_i}{\partial z}\Big|_Z\right) / \Delta Z - \left(\varepsilon_e u \rho_i \Big|_{Z+\Delta Z} - \varepsilon_e u \rho_i \Big|_Z\right) / \Delta Z \quad (4.1.6)$$

Taking limit $\Delta Z \to 0$ gives:

$$\varepsilon_e \frac{\partial \rho_i}{\partial t} + (1-\varepsilon_e) \frac{\partial \rho_s}{\partial t} = \frac{\partial \varepsilon_e D_L}{\partial z} \frac{\partial \rho_i}{\partial z} - \frac{\partial \varepsilon_e u \rho_i}{\partial z} \quad (4.1.7)$$

$$\varepsilon_e \frac{\partial \rho_i}{\partial t} + (1-\varepsilon_e) \frac{\partial \rho_s}{\partial t} = D_L \varepsilon_e \frac{\partial^2 \rho_i}{\partial z^2} - \varepsilon_e \frac{\partial u \rho_i}{\partial z} \quad (4.1.8)$$

Dividing by molecular weight of ith component

$$\varepsilon_e \frac{\partial C_i}{\partial t} + (1-\varepsilon_e)\frac{\partial C_s}{\partial t} = D_L \varepsilon_e \frac{\partial^2 C_i}{\partial z^2} - \varepsilon_e \frac{\partial u C_i}{\partial z} \tag{4.1.9}$$

$\frac{\partial C_s}{\partial t}$ = Mass transfer of solute from bulk solution to the surface of the packing

$$= k_i a_p (C_i - C_{pi}) \tag{4.1.10}$$

This gives:

$$\varepsilon_e \frac{\partial C_i}{\partial t} + \varepsilon_e \frac{\partial (u C_i)}{\partial z} = \varepsilon_e D_L \frac{\partial^2 C_i}{\partial z^2} - (1-\varepsilon_e) k_i a_p (C_i - C_{pi}) \tag{4.1.11}$$

Material balance of ith component in solid phase

From material conservative law:

Accumulation in the pore and adsorbed on the surface	=	Mass transfer from bulk solution to the surface of the packing

Accumulation in the pore (in liq.): $\varepsilon_p V_p \frac{\partial C_{pi}}{\partial t}$ (4.1.12)

Accumulation of the solute adsorbed on the surface: $(1-\varepsilon_p) V_p \frac{\partial \Gamma_i}{\partial t}$ (4.1.13)

Mass transfer from bulk solution to the surface of the packing: $V_p k_i a_p (C_i - C_{pi})$ (4.1.14)

We now add up the contributions to the material balance;

$$\varepsilon_p V_p \frac{\partial C_{pi}}{\partial t} + (1-\varepsilon_p) V_p \frac{\partial \Gamma_i}{\partial t} = V_p k_i a_p (C_i - C_{pi}) \tag{4.1.15}$$

This gives:

$$\varepsilon_p \frac{\partial C_{pi}}{\partial t} + (1-\varepsilon_p) \frac{\partial \Gamma_i}{\partial t} = k_i a_p (C_i - C_{pi}) \tag{4.1.16}$$

Adsorption equilibrium relationship for ith component (Linear Isotherm)

Linear isotherm can be applied for adsorption relations between the adsorbate and solid surface in the dilute system of HPLC. The linear isotherm is defined by

$$\Gamma_i = K_i C_{pi} \tag{4.1.17}$$

where Γ_i = Adsorbed phase concentration [kmol/m^3]

C_{pi} = Concentration in the macropore [kmol/m^3]

K_i = Equilibrium constant [-]

Initial conditions

t = 0; 0<z<L

$$c_i = c_i^0(z) \tag{4.1.18}$$

$$c_{pi} = c_{pi}^0(z) \tag{4.1.19}$$

Boundary conditions

For t>0; z = 0

$$c_i(0) = C_{fi}$$

$$c_{fi} = \begin{cases} c_{fi} & for \;\; t \in [0, t_p] \\ 0 & for \;\; t > t_p \end{cases} \tag{4.1.20}$$

For t > 0; z = L

$$\frac{\partial c_i}{\partial z} = 0 \tag{4.1.21}$$

After introducing dimensionless groups defined as follows:

$$x = \frac{z}{L}; \qquad \tau = \frac{tu_r}{L}; \qquad y_i = \frac{C_i}{\rho_r}; \qquad y_{pi} = \frac{C_{pi}}{\rho_r};$$

$$Pe = \frac{u_r d_p}{D_L}; \qquad St = \frac{k_i a_p L}{u_r}; \qquad \xi = \frac{u}{u_r}; \qquad q_i = \frac{\Gamma_i}{\rho_r};$$

The dimensionless form of the model (4.1.11,4.1.16-4.1.21) reads:

$$\frac{\partial y_i}{\partial \tau} + \frac{\partial (\xi y_i)}{\partial x} = \frac{1}{Pe}\frac{d_p}{L}\frac{\partial^2 y_i}{\partial x^2} - \frac{1-\varepsilon_e}{\varepsilon_e} St\,(y_i - y_{pi}) \tag{4.1.22}$$

$$\varepsilon_p \frac{\partial y_{pi}}{\partial \tau} + (1-\varepsilon_p)\frac{\partial q_i}{\partial \tau} = St_i (y_i - y_{pi}) \tag{4.1.23}$$

$$q_i = K_i y_{pi} \tag{4.1.24}$$

The initial and boundary conditions are

: Initial conditions $\tau = 0$; $0<x<1$

$$y_i = y_i^0(x) \tag{4.1.25}$$

$$y_{pi} = y_{pi}^0(x) \tag{4.1.26}$$

: Boundary conditions for $\tau>0$; $x = 0$

$$y_i(0) = y_{fi}$$

where,

$$y_{fi} = \begin{cases} y_{fi} \; for \;\; \tau \in [0, \tau_p] \\ 0 \;\; for \;\; \tau > \tau_p \end{cases} \tag{4.1.27}$$

For $\tau>0$; $x=1$

$$\frac{\partial y_i}{\partial x} = 0 \tag{4.1.28}$$

4.2 Numerical Method for Solution of Mathematical Model for High Performance Liquid Chromatography

The resulting dimensionless equations are linear and solvable by finite difference techniques, combining with the 4^{th} order Runge-Kutta integration method. After applying numerical method, the solution can be solved directly using functions in MATLAB (version 5.3.1)

CHAPTER 5

Estimation of Modeling Parameters and Conversion Signal

5.1 Estimation of Modeling Parameter

It can be seen from equations (4.1.22-4.1.28 in section 4.1 in Chapter 4) that the mathematical description of the chromatographic column contains some model parameters to be estimated. These are internal porosity, ε_p, external porosity (bed porosity), ε_e, the axial dispersion coefficient, D_L, adsorption isotherms, $\Gamma(c)$, and the overall mass transfer coefficient, k. BET and Pore Sizer can estimate the internal porosity. Axial dispersion is calculated from semiempirical relationship for packed-beds. Adsorption equilibrium can be obtained from the first moment analysis. Each parameter can be estimated by the following method in this chapter.

5.1.1 Internal Porosity

Internal porosity can be estimated from specific pore volume, V_p, and particle density, ρ_p, as the following equation.

$$\varepsilon_p = V_p \rho_p \qquad (5.1.1.1)$$

The specific pore volume, V_p, is measured by BET and particle density, ρ_p, is measured by Pore Sizer.

5.1.1.1 Procedure for the Estimation of Internal Porosity

1. Three hundred milligrams of packing material were used to determine bulk density by Pore Sizer model Micromeritics ASAP 2.000 and pore volume by BET (Brunauer, Emmett, and Teller) model Micromeritics PoreSizer 9320. The analysis is performed at ambient temperature (the maximum limit of temperature for the packing material is 40°C).
2. The internal porosity is estimated according to Equation 5.1.1.1.

5.1.1.2 Results for the Estimation of Internal Porosity

The average of specific pore volume, V_p, measured by BET is 0.4983 cm^3/g and the average particle density, ρ_p, measured by Pore Sizer is 0.5184 g/cm^3. The BET and Pore Sizer experiments are performed in duplicate. Internal porosity is estimated to be 0.2583.

5.1.2 External Porosity

The external porosity, ε_e, can be estimated by injection of nonadsorbable macromolecule into the HPLC column at various flow rates of mobile phase. In this case blue dextran (M.W. 1,000,000), is used as a solute. The solute is injected at 5 different flow rates (0.4, 0.6, 0.8, 1.0, and 1.2 ml/min). The bed voidage, ε_e, can be calculated from the time of the peak maximum, t_{max}, for symmetric peaks.

$$\varepsilon_e = \frac{Q}{V_{total}} \cdot t_{max} \qquad (5.1.2.1)$$

5.1.2.1 Procedure for the Estimation of External Porosity

1. Prepare pulse tracer, blue dextran solution, at 0.2 mg/ml by dissolving blue dextran in methanol 33% aqueous solution.
2. Filter each blue dextran sample through 0.2 PTFE microfilters.
3. Auto inject 10 µl of each blue dextran sample at 5 different flow rates of the selected mobile phase: 0.6, 0.8, 0.9, 1.0, 1.2, 1.4 ml/min. The UV spectra is recorded with the recorder.
4. Determine the external porosity according to Equation 5.1.2.1.

5.1.2.2 Results for the Estimation of External Porosity

External porosity can be estimated from a slope of a plot of t_{max} versus V_{total} / Q according to Equation (5.1.2.1):

$$\varepsilon_e = \frac{Q}{V_{total}} \cdot t_{max}$$

Figure 5.1.2.1 shows the relationship between t_{max} and $\frac{V_{total}}{Q}$. The plot of t_{max} versus $\frac{V_{total}}{Q}$ is a straight line through the origin with the least square error rather than 0.99. The external porosity can be obtained from the slope of the plot according to Equation (5.1.2.1). External porosity can estimated to be 0.3508

5.1.3 Adsorption Equilibrium

At sufficient low concentration of adsorbate, Linear isotherm can be applied for the prediction of concentration profiles in HPLC column. Equilibrium constant, K_i, are estimated from the first moment analysis.

$$t_{max} = [\varepsilon_e + (1-\varepsilon_e)(\varepsilon_p + K_i)]\frac{V_{total}}{Q} \quad (5.1.3.1)$$

5.1.3.1 Procedure for the Estimation of Adsorption Equilibrium

1. Perform pulse response experiments with 5 different flow rates (0.8, 0.9, 1.0, 1.2, 1.4 ml/min).
2. With ε_e and ε_p values obtained from section 5.1.1 and 5.1.2, determine the adsorption equilibrium according to Equation (5.1.3.1).
3. Repeat the experiments with different concentration varied from 0.009 to 0.072 mg/ml for daidzin and 0.004 to 0.016 mg/ml for genistin.

5.1.3.2 Results for the Estimation of Adsorption Equilibrium

For the experiments presented here, linear isotherm is applied for the system, considering the concentration of adsorbate in HPLC system is diluted. From the experiments, the retention time remains constant as the concentration of samples (daidzin and genistin) increases. Therefore, the adsorption isotherm for daidzin and genistin is well expressed as linear isotherm. Figure 5.1.3.1 and Figure 5.1.3.2 show the plot of t_{max} versus $\frac{V_{total}}{Q}$ of daidzin and genistin at various concentration, respectively. The adsorption equilibrium, K, can be estimated from the slope of the plot of t_{max} and $\frac{V_{total}}{Q}$, according to Equation (5.1.3.1).

The adsorption equilibrium of daidzin and genistin are estimated to be 5.1015 and, 10.7868, respectively. Hence following linear isotherm is obtained:

Linear isotherm of daidzin:

$$q_d = 5.1015\, y_{p,d} \qquad (5.1.3.2)$$

where q_d = Dimensionless adsorbed phase concentration of daidzin

$y_{p,d}$ = Dimensionless concentration in the macropore of daidzin

Linear isotherm of genistin:

$$q_g = 10.7868\, y_{p,g} \qquad (5.1.3.3)$$

where q_g = Dimensionless adsorbed phase concentration of genistin

$y_{p,g}$ = Dimensionless concentration in the macropore of genistin

5.1.4 Axial Dispersion Coefficient

The axial dispersion coefficient is estimated by the semiempirical correlation proposed by Chung and Wen, 1968

$$\varepsilon_e Pe = 0.2 + 0.011\, Re^{0.48} \qquad (5.1.4.1)$$

where Pe = Peclet's number $= \dfrac{u_r d_p}{D_L}$

Re = Reynold's number $= \dfrac{\rho u d_p}{\eta}$

Table 5.1 Axial dispersion coefficient at 3 different flow rates of mobile phase

Flow rate [ml/min]	Reynold Number	Axial Dispersion Coefficient
0.8	6.014E-3	4.3644E-8
1.0	7.517E-3	4.3621E-8
1.4	1.052E-2	4.3581E-8

5.1.5 Mass Transfer Coefficients

The mass transfer coefficient, k , was used as an adjustable parameter to fit the experimental data. The best-fit value of this parameter was estimated by calculating the sum of squared error between the predicted and measured values at the column outlet for each time step.

Estimated modeling parameters, the internal porosity, ε_p , the external porosity, ε_e , the adsorption equilibrium, K , the axial dispersion coefficient, D_L , are summarized in Table 5.2.

Table 5.2 Modeling parameters, the internal porosity, ε_p , the external porosity, ε_e , the adsorption equilibrium, K , the axial dispersion coefficient, D_L

	Daidzin	**Genistin**
Internal Porosity (ε_p)	0.2583	
External Porosity (ε_e)	0.3508	
Adsorption Equilibrium (K)	5.1015	10.7868
Axial Dispersion Coefficient (D_L)	Shown in Table 5.1	

5.2 Estimation of Extinction Coefficient

Signal of the chromatograms recorded by UV-HPLC detector is in absorbance unit. Before further applying to compare with simulation results, absorbance unit must be converted into concentration unit following Beer and Lambert's law.

$$AU = \varepsilon \times \ell \times C_i \qquad \text{(Beer and Lambert's law)} \qquad (5.2.1)$$

where,

AU = Absorbance Unit [AU]
ε = Extinction Coefficient [AU/m-g/l]
ℓ = Light Path Length [m]
C_i = Concentration [g/l]

The extinction coefficient of any substance can be determined based on experiments using UV-visible spectrophotometer.

5.2.1 Procedure for the Estimation of Extinction Coefficient

1. Prepare Daidzin sample at 4 different concentration: 0.003125, 0.006250, 0.012500, and 0.02500 mg/ml in ethanol 70% aqueous solution and Genistin at 3 different concentration: 0.003125, 0.006250, and 0.02500 mg/ml in ethanol 70% aqueous solution.
2. Record the absorbance of each sample by UV-visible spectrophotometer model Thermo Spectronic HEλIOS.
3. Determine the extinction coefficient according to Equation 5.2.1.

5.2.1 Results for the Estimation of Extinction Coefficient

Figures 5.2.1, and 5.2.2 show the plot of absorbance unit versus concentration of daidzin and genistin, respectively. The plots demonstrate respective linear relationships for all data points with least square error rather than

0.9999. The slope of each line is the multiple of the extinction coefficient (ε) and the light path length (ℓ). The light path length of the UV-visible spectophotometer and UV-detector is 0.01 m. Therefore, the extinction coefficients of daidzin and genistin is 7,178.9 and 18,584 AU/m-g/l, respectively. The values of the extinction coefficient obtained from the plots are used for the conversion of absorbance unit into the concentration unit for this research.

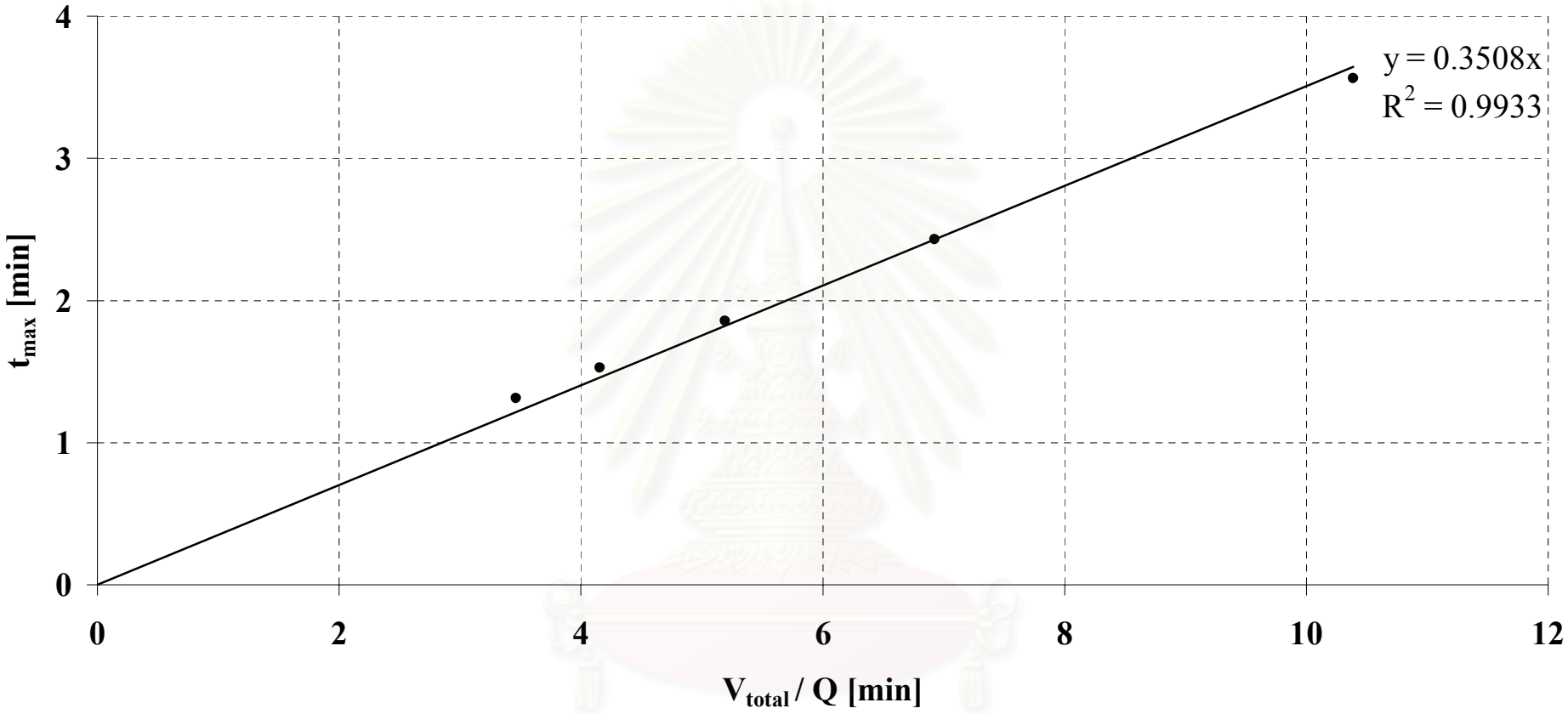

Figure 5.1.2.1 The relationship between t_{max} and V_{total}/Q of blue dextran

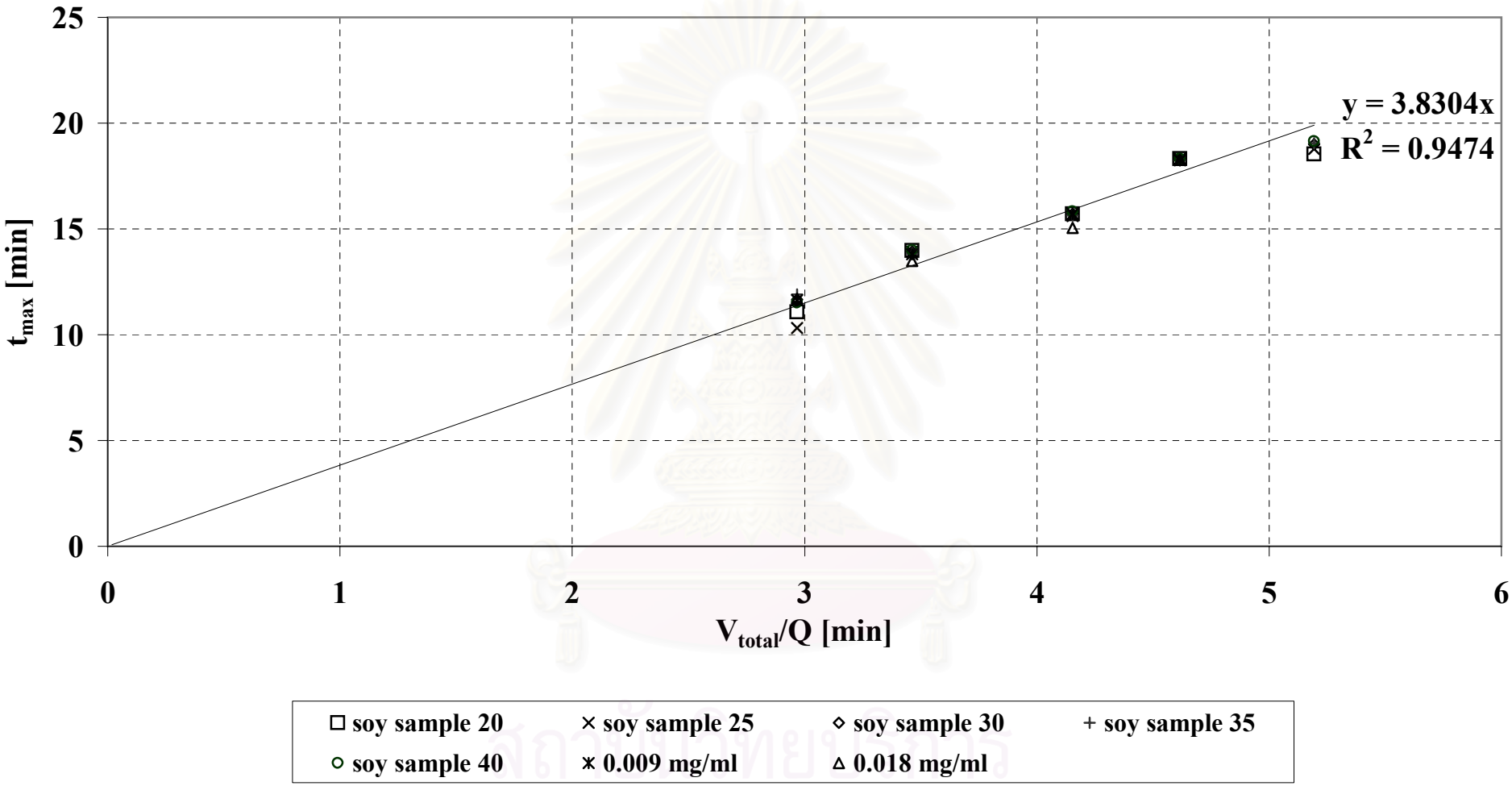

Figure 5.1.3.1 The relationship between t_{max} and V_{total}/Q of daidzin

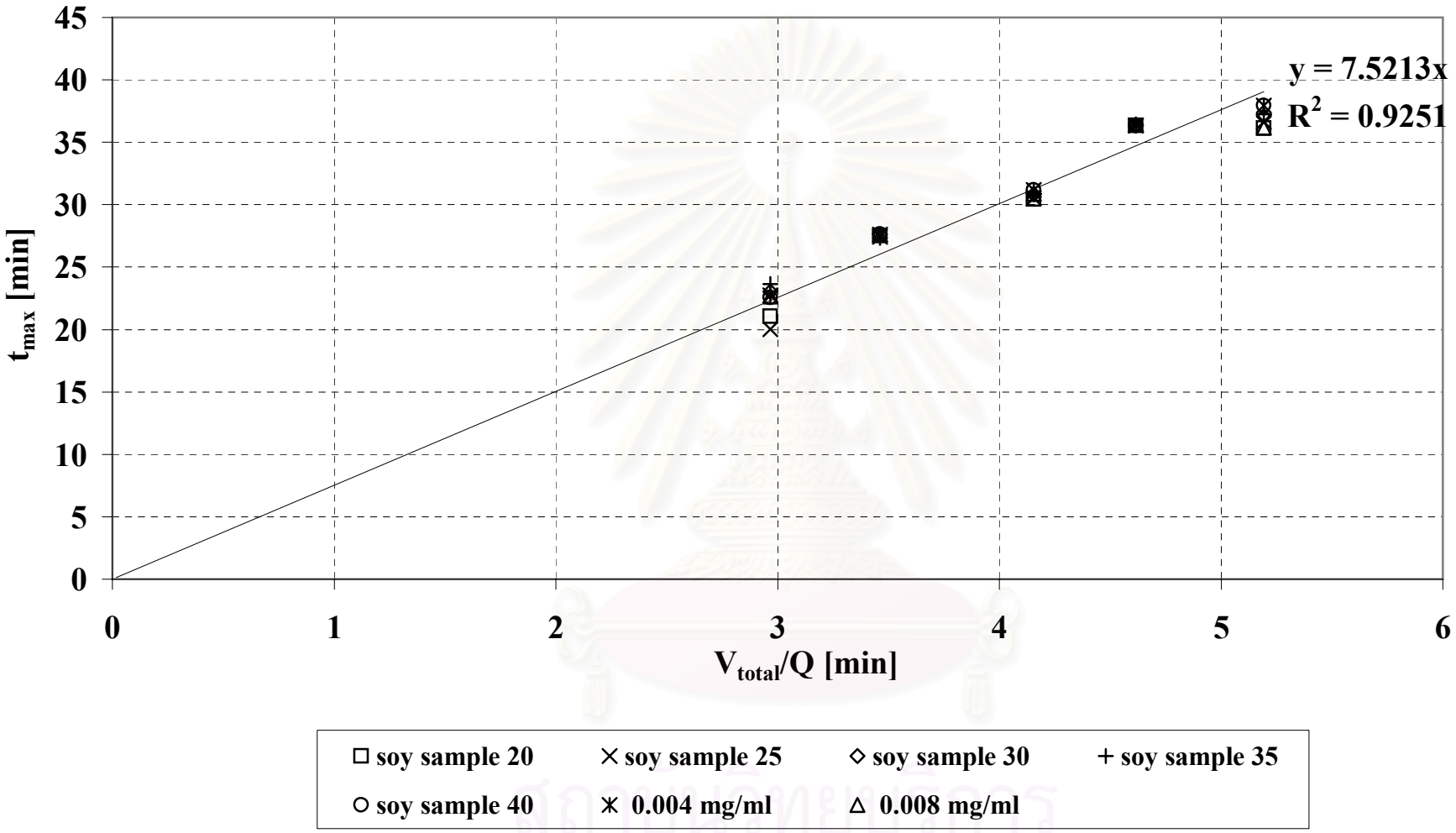

Figure 5.1.3.2 The relationship between t_{max} and V_{total}/Q of genistin

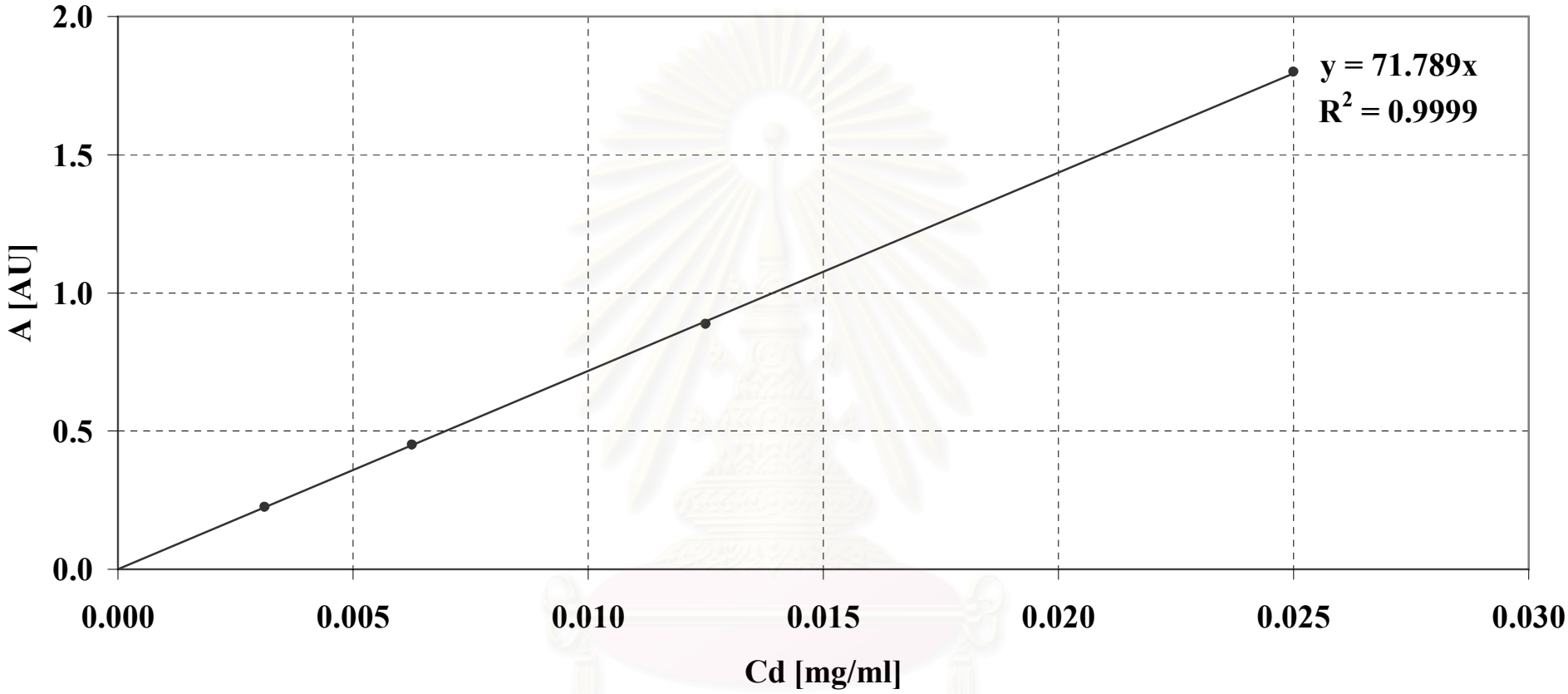

Figure 5.2.1 Plot of the Absorbance, A, against the concentration of daidzin, Cd, from UV-visible spectrophotometer

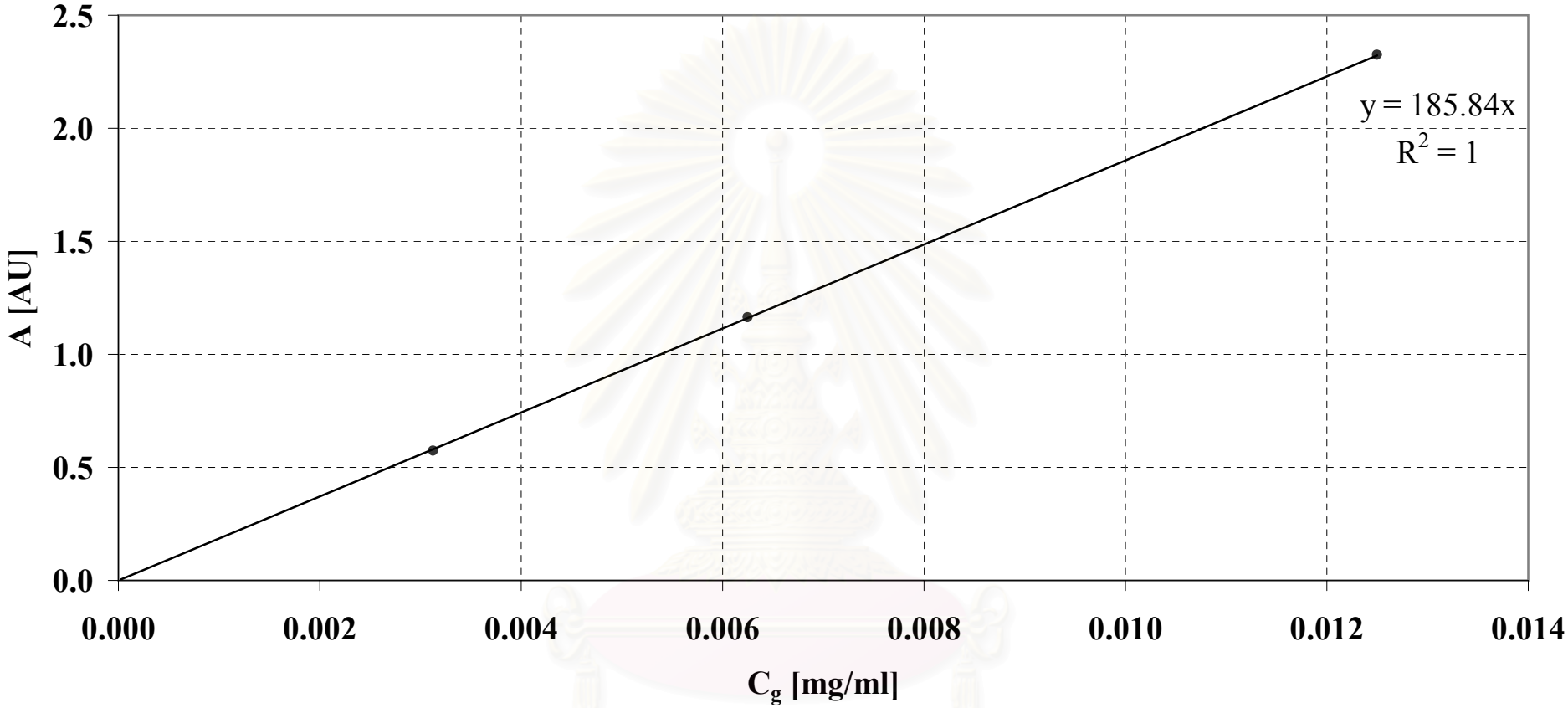

Figure 5.2.2 Plot of the Absorbance, A, against the concentration of genistin, Cg, from UV-visible spectrophotometer

CHAPTER 6

Results and Discussion

6.1 Mobile Phase for the Separation

Solvents that are commonly used as mobile phase in analysis of isoflavones from soybean flake extracts by HPLC are acetonitrile, methanol, and ethanol (West et al., 1978; Murphy, 1981; Eldridge, 1982; Wang et al., 1990; Coward et al. 1993; Barnes, Kirk, and Coward, 1994; Wang and Murphy, 1996; Song et al., 1998; Hutabarat et al., 1998; Choi, and Row, 2000). Even though acetonitrile-water was used commonly, it was believed to have carcinogenic risk to humans. Hence acetonitrile-water was not suitable to use as the mobile phase to separate isoflavones for production into drug forms or health supplements. From the experimental study with ethanol-water at different concentrations as the mobile phase, the resolution of the separations was not satisfactory; isoflavone peaks could not be isolated. Therefore, the mixture of methanol-water was selected as the mobile phase. Methanol-water at suitable combination produced the good resolution for isoflavone separation. Daidzin and genistin could be isolated from other components in soybean flake extracts. Figure 6.1(a) – Figure 6.1(h) show the chromatograms of isoflavones in soybean flake extracts at various concentrations of methanol in water i.e. 25%, 30%, 33%, 35%, 37%, 38%, 39%, and 40%. The more percentage of methanol in mobile phase, the less run time was observed. However, Daidzin and genistin could not be truly isolated from others by methanol more than 40 % aqueous solution. The optimum concentration of methanol that can totally separate daidzin and genistin from other components with the minimum run time is 33% aqueous solution. Therefore, in the following studies, 33% methanol aqueous solution was used as the mobile phase. The separation of isoflavones in the Analytical Reverse-Phase HPLC with different mobile phases was summarized in Table 6.1. The resolution in the Table 6.1 is defined by the ratio of difference in residence time to the average peak width.

Table 6.1 The summary of isoflavones separation in the Analytical Reverse-Phase HPLC with different mobile phases

Type of Mobile phase	Component	Retention time [min]	Resolution; R_{d3}[a]	Resolution; R_{d4}[a]	Resolution; R_{g4}[a]
Ethanol	Isoflavones could not be separated				
Acetonitrile (gradient)	daidzin	No data			
	genistin				
Methanol 25%	daidzin	24.908	-	-	-
	genistin	44.675	-	-	-
Methanol 30%	daidzin	21.608	3.527	2.977	-
	genistin	43.792	-	-	5.672
Methanol 33%	daidzin	15.305	1.532	2.426	-
	genistin	29.788	-	-	6.209
Methanol 35%	daidzin	12.538	1.006	1.434	-
	genistin	23.538	-	-	4.442
Methanol 37%	daidzin	10.352	-	1.171	-
	genistin	18.868	-	-	4.364
Methanol 38%	daidzin	9.812	0.781	0.941	-
	genistin	17.812	-	-	4.138
Methanol 39%	daidzin	9.915	0.816	0.765	-
	genistin	15.412	-	-	3.6645
Methanol 40%	daidzin	7.623	0.882	0.6147	-
	genistin	12.195	-	-	3.1918

[a] : d denotes daidzin, g denotes genistin, 3 denotes peak no. (3) in the Figure 6.1(a) to Figure 6.1(h), 4 denotes peak no. (4) in the Figure 6.1(a) to Figure 6.1(h)

6.2 Calculation of the Dead Time for HPLC System

The HPLC column is connected to the autosample injector and the detector with small tubes as shown in Figure 3.1 in chapter 3. Solvent delivery through these tubes required some time called *dead time,* t_{de} . Dead time can be calculated from the following equation.

$$t_{de} = \frac{L_t \times A_t}{Q} \qquad (6.2.1.1)$$

where,

L_t = Length of tube connecting HPLC column and autosample injector and UV detector [m]

A_t = Crossectional area of tube connecting HPLC column with autosample injector and UV detector [m^2]

Q = Volumetric flow rate [m^3/s]

Time recorded by the detector must be subtracted by the dead time before further calculation. Table 6.2 shows the dead time of each flow rate.

Table 6.2. Dead time of each flow rate

Flow rate of mobile phase [ml/min]	Dead time [min]
0.8	0.061
0.9	0.054
1.0	0.049
1.2	0.041
1.4	0.035

6.3 Calculation of the Concentration at the Inlet of the HPLC Column

HPLC involves injecting a pulse of sample into the column. The injected sample is then diluted when it is delivered by mobile phase. Concentration of the components at the inlet of HPLC column has to be determined to provide the initial condition for the simulation. From material balance, the inlet concentration can be approximately calculated from the following equation.

$$C_f = \frac{C_j \times V_j}{t_p \times Q} \qquad (6.4.1.1)$$

where,

C_f = Concentration at the inlet HPLC column [kmol/m^3]

C_j = Concentration of daidzin or genistin in the soybean flake extracts sample [kmol/m^3]

V_j = Injection volume [m^3]

t_p = Time during the constant concentration C_f is fed into column [s]

6.4 Revision of the Internal Porosity and the Adsorption Equilibrium Constant

The internal porosity, ε_p, the external porosity, ε_e, the adsorption equilibrium constant, K, and the axial dispersion coefficient, D_L, are estimated as shown in Table 5.2 in chapter 5. These modeling parameters are applied in the simulations without dispersion term (the program #1 as in Appendix A) for investigation of their accuracy without accounting for the axial dispersion coefficient. The axial dispersion term is not covered in this simulation because it requires less CPU time than the simulation which axial dispersion is covered. Other necessary parameters are given in caption to figures.

Figure 6.4.1 shows the comparison between the experimental data and the simulation result of daidzin. The experiment is performed at the flow rate of 1.0 ml/min and at the concentration of 0.072 mg/ml. The retention time of daidzin in the experiment and the simulation is 15.25, and 15.98 minutes, respectively. The difference between elution times obtained from the experiment and the simulation implied the error of the estimated parameter that affects the retention time, which is the adsorption equilibrium. Therefore, the internal porosity is reconsidered by means of trial and error. As shown in Figure 6.4.2, the retention time of the experimental data and the simulation results are the same when the internal porosity is 0.05. With the adjusted internal porosity value, the adsorption equilibrium of daidzin calculated from Equation 5.1.3.1 in section 5.1.3 in chapter 5 is 5.3098.

Regarding the internal porosity is nearly zero, only small amount of isoflavones was adsorbed in the internal pore. From Gugger et al. (1997), ultrafiltration membrane was used to separate isoflavones in the soybean flake extracts. It was found that nearly 50% of isoflavones (daidzin, and genistin) could not pass through the membrane. Therefore, the size of daidzin and genistin could be in the range of the size of the packing pore diameter (100 Å). Hence almost of daidzin and genistin molecules can not diffuse into the pore of the packing. The estimated parameter from the revision accords well with the expectation from the comparison between the size of adsorbate and the pore size of packing material. Figure 6.4.3 shows the experimental data and the simulation result of genistin at flow rate of 1.0 ml/min and concentration of 0.016 mg/ml. By trial and error of the internal porosity with genistin data, the internal porosity for the simulation of genistin is 0.05 and the adsorption equilibrium is 10.9951. The values of internal porosity and the adsorption equilibrium from the revision are summarized in Table 6.3.

Table 6.3 The internal porosity and the adsorption equilibrium from the revision

	Daidzin	Genistin
Internal Porosity	0.05	0.05
Adsorption Equilibrium	5.3098	10.9951

6.5 Comparison between Results from the Simulation with and without Axial Dispersion Term.

After the external porosity, ε_e, the internal porosity, ε_p, the adsorption equilibrium, K, and the axial dispersion coefficient, D_L, were revised as in the section 6.4, these model parameters are applied for the simulation with dispersion term (the program #2 in Appendix A). Figure 6.5.1 shows the comparison between the simulated results and the experimental data. Figure 6.5.1(a) and Figure 6.5.1(b) are obtained from the simulation with and without the axial dispersion coefficient. Squares in the figure represent the result of the experiment and solid line represents the calculations from the program with the axial dispersion. The measure of the quality of the fit as the mean squared error (mse) was 1.932E-9. Plots shown in Figure 6.5.1(a) were obtained after 4680 minutes of calculation. As it is shown the computation required large amount of times. The elimination the axial dispersion term was proposed by Rouchon et al. (1987) and used by Czok and Guiochon (1990 a, b) and Ma and Guiochon (1991). These authors showed that the effect caused by the axial dispersion term in a material balance equation could be the same as the simulation, which the axial dispersion term is neglected if the space and time increments of the finite different method are properly. Figure 6.5.1(b) shows the comparison between the simulated results and the experimental data in the program without the axial dispersion term (the program #1 in Appendix A). Squares in the figure represents the result of the experiment and solid line represents the calculations from the program without the axial dispersion. From the comparison, the mean squared error was 8.209E-9. Plots shown in Figure 6.5.1(b) were obtained after 480 minutes of calculation. Although the results obtained by the two methods (simulations with and without dispersion terms) yielded almost the same accuracy, the CPU time was from eight to nine times shorter for the simulation without the axial dispersion term. Hence the simulation without the axial dispersion term was used for the simulation of the following studies.

6.6 Estimation of the Mass Transfer Coefficient

After the external porosity, ε_e , the internal porosity, ε_p , and the adsorption equilibrium, K , were revised as in the section 6.4, the mass transfer coefficient, k , is estimated by trial and error. Figures 6.4.2 to 6.4.3 show the comparison between the experimental data and the simulation results of daidzin and genistin, respectively. The experimental data are performed at 0.072 mg/ml of daidzin and 0.016 mg/ml of genistin at flow rate of mobile phase 1 ml/min. The mass transfer coefficient of daidzin and genistin at flow rate of mobile phase 1 ml/min that fit the experimental data are 5.333E-5, and 5.833E-5 m/s, respectively. The mean square error of both daidzin simulation and genitin simulation is less than 1E-8. To estimate the mass transfer coefficient at other flow rates, the correlation of mass transfer coefficient by Wilson and Geankoplis (1966) is used. From the correlation, mass transfer coefficient is the function of Reynold number in power of 0.33 $\left(k = \frac{1.09 D_{mi}}{d_p \varepsilon_e} Re^{0.33} Sc^{0.33} \right)$. Hence the mass transfer coefficient at other flow rates can be estimated by the mass transfer coefficient at flow rate 1 ml/min. Table 6.4 shows the mass transfer coefficient at various flow rates of the mobile phase.

Table 6.4. The mass transfer coefficient at various flow rates of mobile phase

Flow rate [ml/min]	Mass Transfer Coefficient of Daidzin [m/s]	Mass Transfer Coefficient of Genistin [m/s]
0.8	4.955E-5	5.419E-5
1.0	5.333E-5	5.833E-5
1.4	5.959E-5	6.517E-5

Estimated modeling parameters that apply thorough the research are summarized in the following Table.

Table 6.5 Revised modeling parameters, the internal porosity, ε_p, the external porosity, ε_e, the adsorption equilibrium, K, the axial dispersion coefficient, D_L, and the mass transfer coefficient k

Modeling Parameters	Daidzin	Genistin
ε_e	0.3508	
ε_p	0.05	
K	5.3098	10.9951
k	Shown in Table 6.4	
D_L	Shown in Table 5.1	

6.7 Effect of the Injected Sample Concentration on the Simulation

The effect of the injected sample concentration of daidzin and genistin on the simulation is shown in Figures 6.7.1 to 6.7.7. Figures 6.7.1 to 6.7.4 are the comparison between the experimental data and the simulation results of daidzin and genistin in the standard solution and Figures 6.7.5 to 6.7.7 are the comparison between the experimental data and the simulation results of daidzin and genistin in the soybean flake extract solution. All of the experiments are performed at the flow rate of the mobile phase 1.0 ml/min. The modeling parameters used in the simulation are shown in the Table 6.5.

As can be seen, the agreement between the simulation results and the experimental data with various concentrations is relatively good. All of the cases have the mean square error less than 1E-8. Table 6.6 shows the mean square error in each case. It is found that the dispersion term does not affect the accuracy much. In the case of daidzin and genistin in the soybean flake extract solution, the simulation results still agree well with the experimental data. The effect of other components in the soybean extract solution on daidzin and genistin separation is not significant due to the diluted concentration in the HPLC system. From the experimental studies, the shifts of the peak retention time sometime occurred from experimental errors, which

may also cause the difference between the simulation and the experimental data. Overall, the peak height from the profiles of the simulation and the experimental data of daidzin and genistin in the soybean flake extract solution are similar with small imprecision as shown in Figures 6.7.5 to 6.7.7.

Table 6.6 shows the mean square error between the experimental data and the simulation result at the various concentrations

Figure	Sample	Concentration [mg/ml]	Mean Square Error
6.7.1	daidzin	0.072	8.209E-9
6.7.2	daidzin	0.036	3.810E-10
6.7.3	genistin	0.016	1.872E-10
6.7.4	genistin	0.008	5.822E-11
6.7.5	daidzin in soybean extracts	0.018	9.511E-10
	genistin in soybean extracts	0.014	4.348E-10
6.7.6	daidzin in soybean extracts	0.014	2.135E-9
	genistin in soybean extracts	0.010	1.232E-9
6.7.7	daidzin in soybean extracts	0.012	7.009E-11
	genistin soybean extracts	0.009	8.399E-12

6.8 Effect of the Flow Rate on the Simulation

The estimation of modeling parameters was obtained from the experimental data at flow rate 1 ml/min. The effect of mobile phase flow rate variations on the simulation was investigated in this section. Figures 6.8.1 and 6.8.2 show the comparison between the experimental data and the simulation results of daidzin and genistin, respectively at 3 different flow rate; 0.8, 1.0, and 1.4 ml/min. The concentration of daidzin is 0.012 mg/ml and of genistin is 0.010 mg/ml.

It is found that increasing flow rate of the mobile phase results in the faster elution time. The comparison of the profiles in Figure 6.8.1 to 6.8.2 shows that the

simulation results agree well with the experimental data. The estimated mass transfer coefficient obtained in the section 6.6 can give relatively good prediction of isoflavone separation. Table 6.7 show the mean square error in each case

Figures 6.8.3 and 6.8.4 show the comparison between the resident time of the simulation and the resident time of the experiment of daidzin and genistin separation, respectively. It is shown that the predicted time agrees well with the elution time from the experiment.

Table 6.7 show the mean square error between the experimental data and the simulation result at the various flow rates

Figure	Flow Rate [ml/min]	Mean Square Error
6.8.1	0.8	2.425E-10
	1.0	9.511E-10
	1.4	5.969E-9
6.8.2	0.8	8.826E-11
	1.0	4.348E-10
	1.4	9.713E-10

6.9 Determination of the Relationship between the Concentration of Mobile Phase and the Adsorption Equilibrium of Daidzin and Genistin

In this study isoflavones were eluted with methanol-water (33:67 vol/vol) as the mobile phase used isocratically at ambient temperature. With the selected mobile phase, daidzin and genistin can totally separate from other components in soybean flake extract with the run time 30 minutes at flow rate 1 ml/min. Gradient method to adjust the optimum composition of mobile phase during the operation can be further applied to reduce the run time. Even though the gradient method is not covered in this research, the useful data for running gradient are determined. Figures 6.9.1 and 6.9.2 represent the plots between the adsorption equilibrium of daidzin and genistin from

the equation 5.1.3.1 and the concentration of methanol in mobile phase varied from 25 to 40% in aqueous solution. The result shows that the adsorption equilibrium was proportionally linear with the content of water in the mobile phase. The following equations represent the relationship between the adsorption equilibrium of daidzin or genistin and the concentration of methanol in mobile phase.

Daidzin;

$$K_d = -0.426 C_m + 19.212 \quad (6.9.1)$$

Genistin;

$$K_g = -0.787 C_m + 35.899 \quad (6.9.2)$$

where K_d = the adsorption equilibrium of daidzin [-]

K_g = the adsorption equilibrium of genistin [-]

C_m = The percentage of methanol in mobile phase.

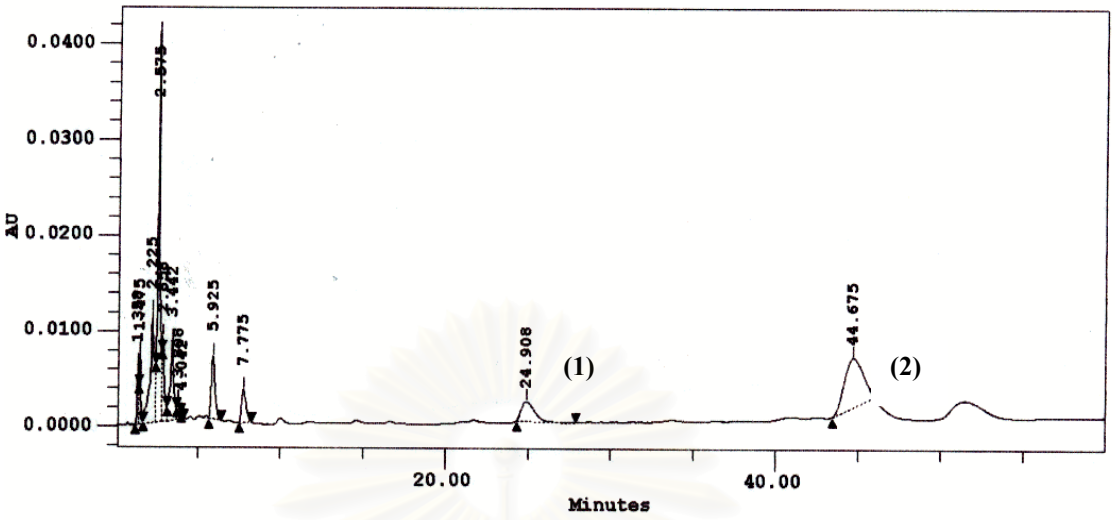

(a)

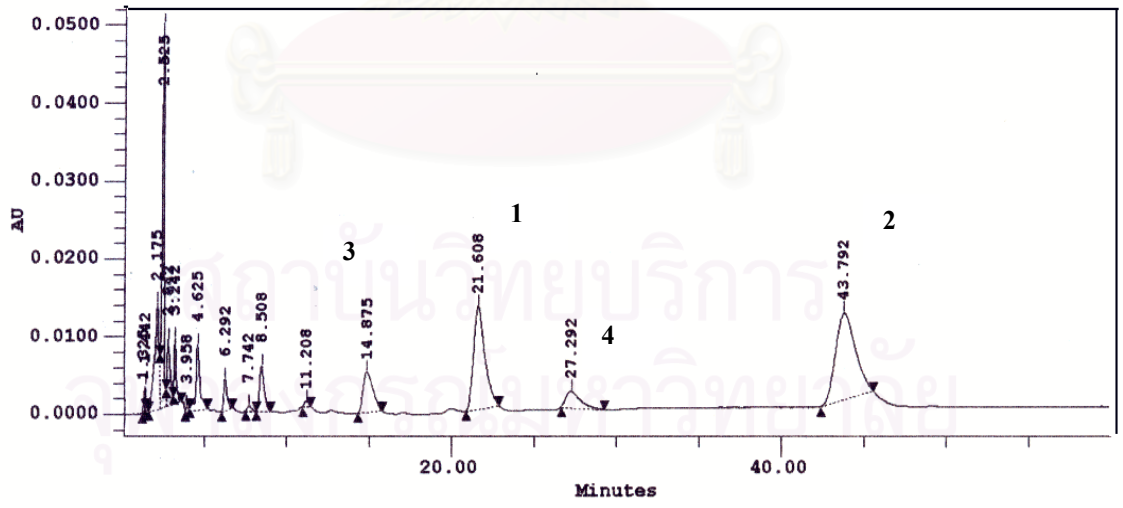

(b)

Figure 6.1 Chromatogram of phytoestrogens in soybean flake extracts: 1, daidzin; 2, genistin with mobile phase (a) methanol 25% and (b) methanol 30% aqueous solution

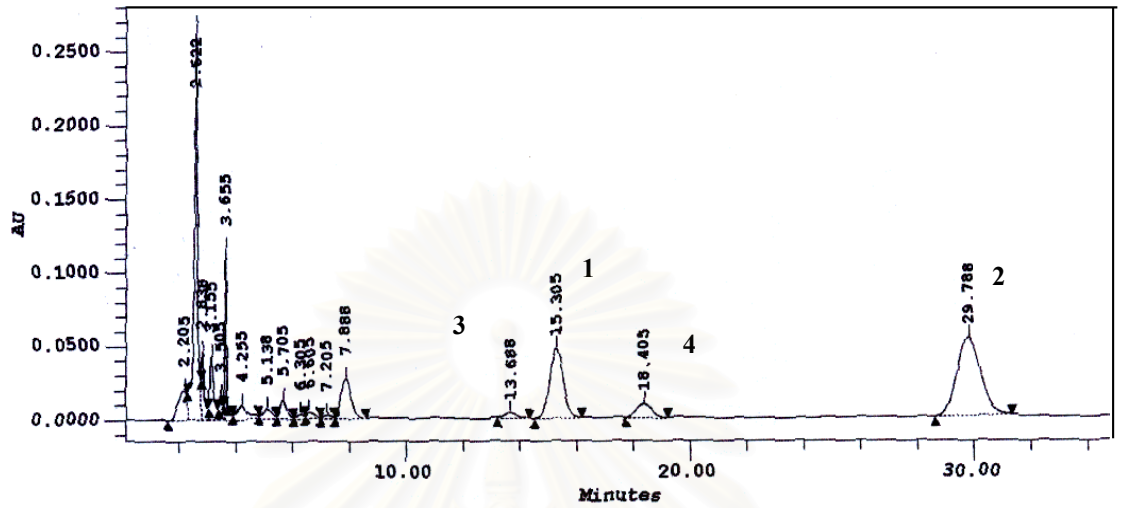

(c)

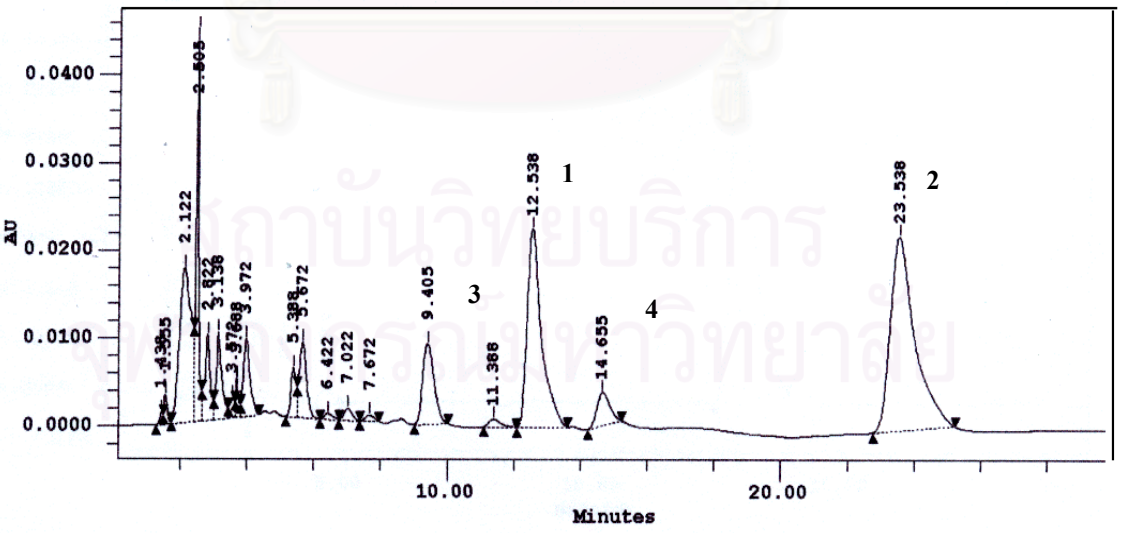

(d)

Figure 6.1 Chromatogram of phytoestrogens in soybean flake extracts: 1, daidzin; 2, genistin with mobile phase (c) methanol 33% and (d) methanol 35% aqueous solution

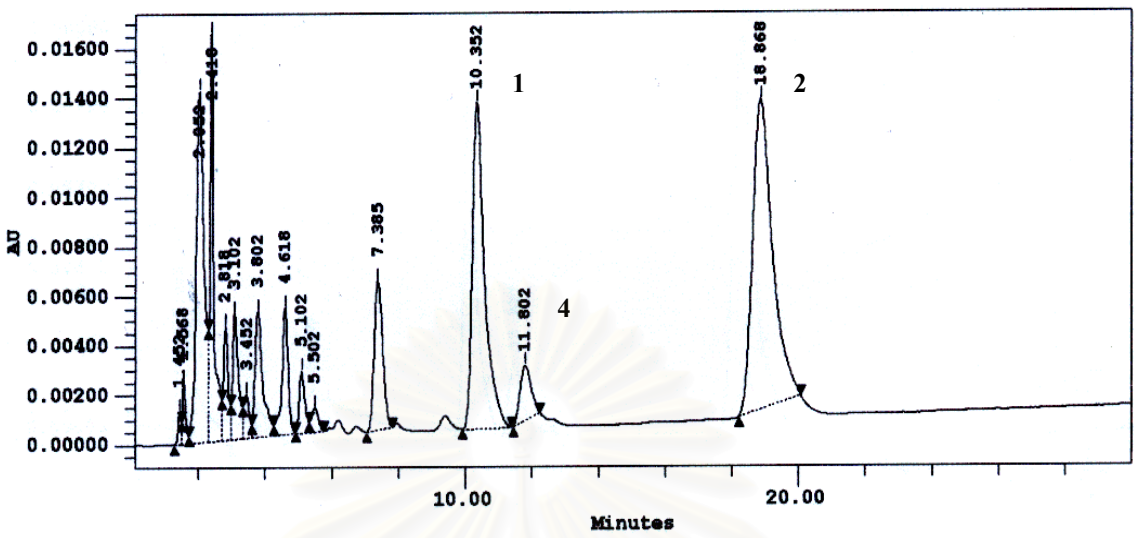

(e)

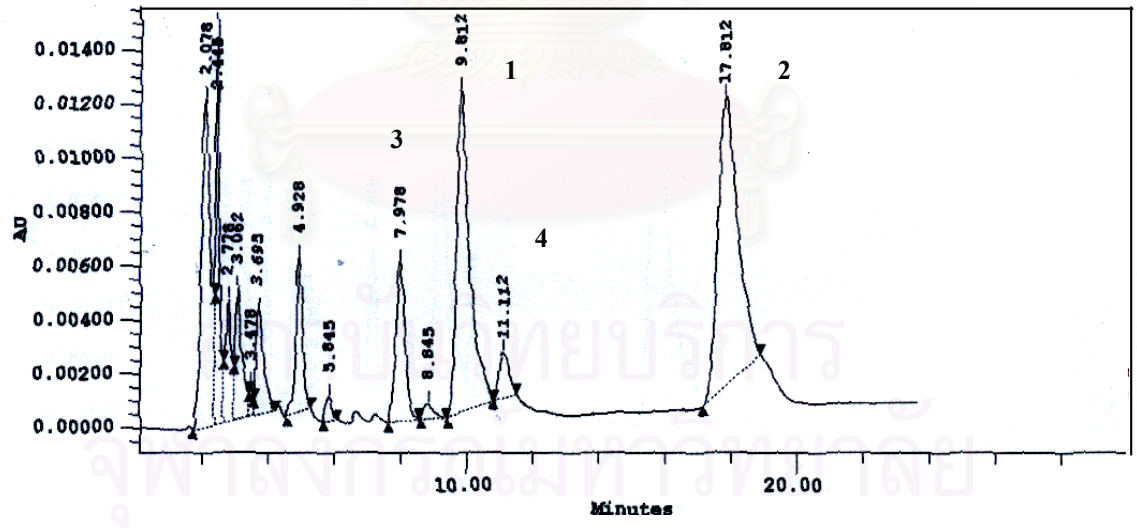

(f)

Figure 6.1 Chromatogram of phytoestrogens in soybean flake extracts: 1, daidzin; 2, genistin with mobile phase (e) methanol 37% and (f) methanol 38% aqueous solution

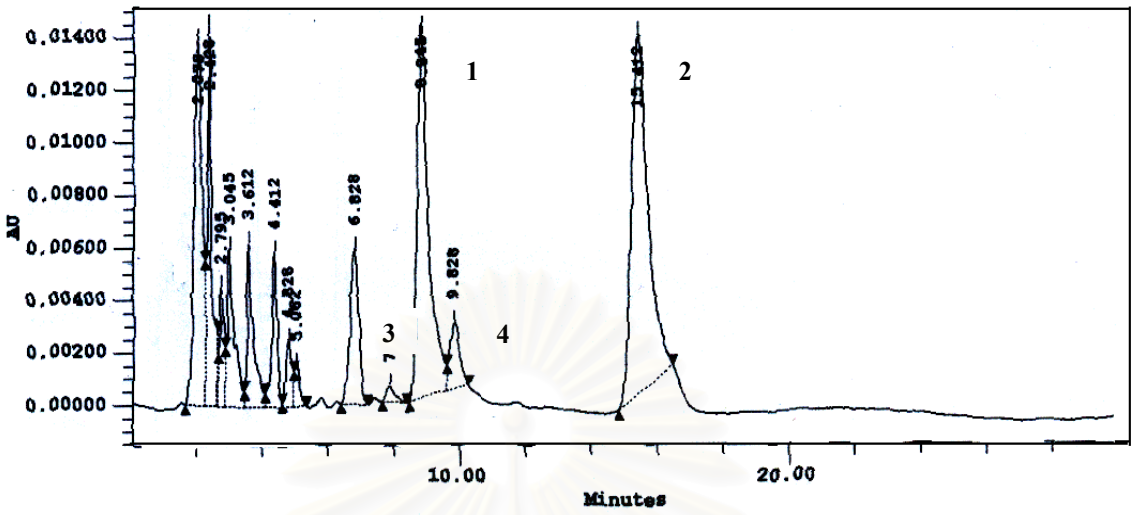

(g)

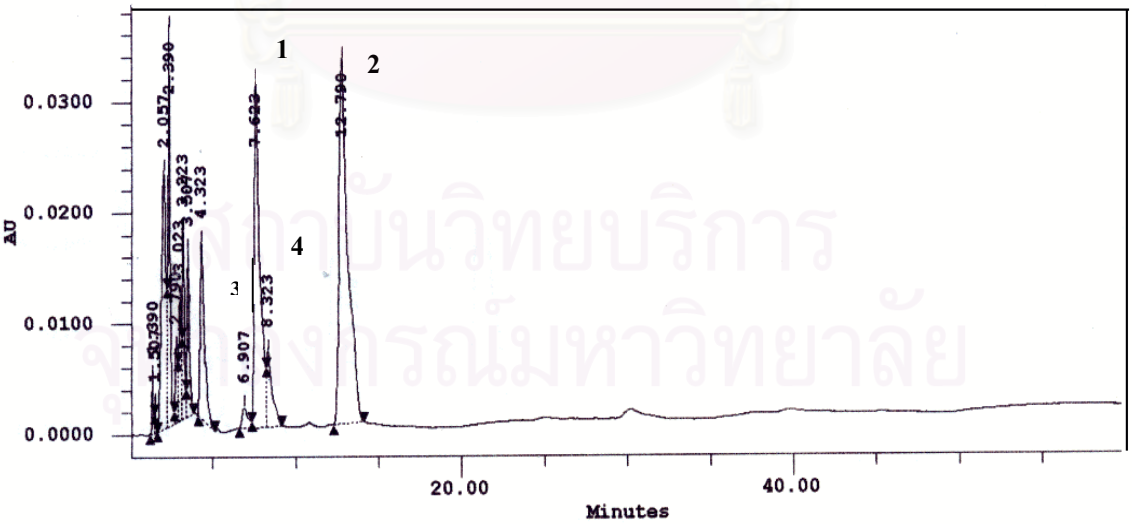

(h)

Figure 6.1 Chromatogram of phytoestrogens in soybean flake extracts: 1, daidzin; 2, genistin with mobile phase (g) methanol 39% and (h) methanol 40% aqueous solution

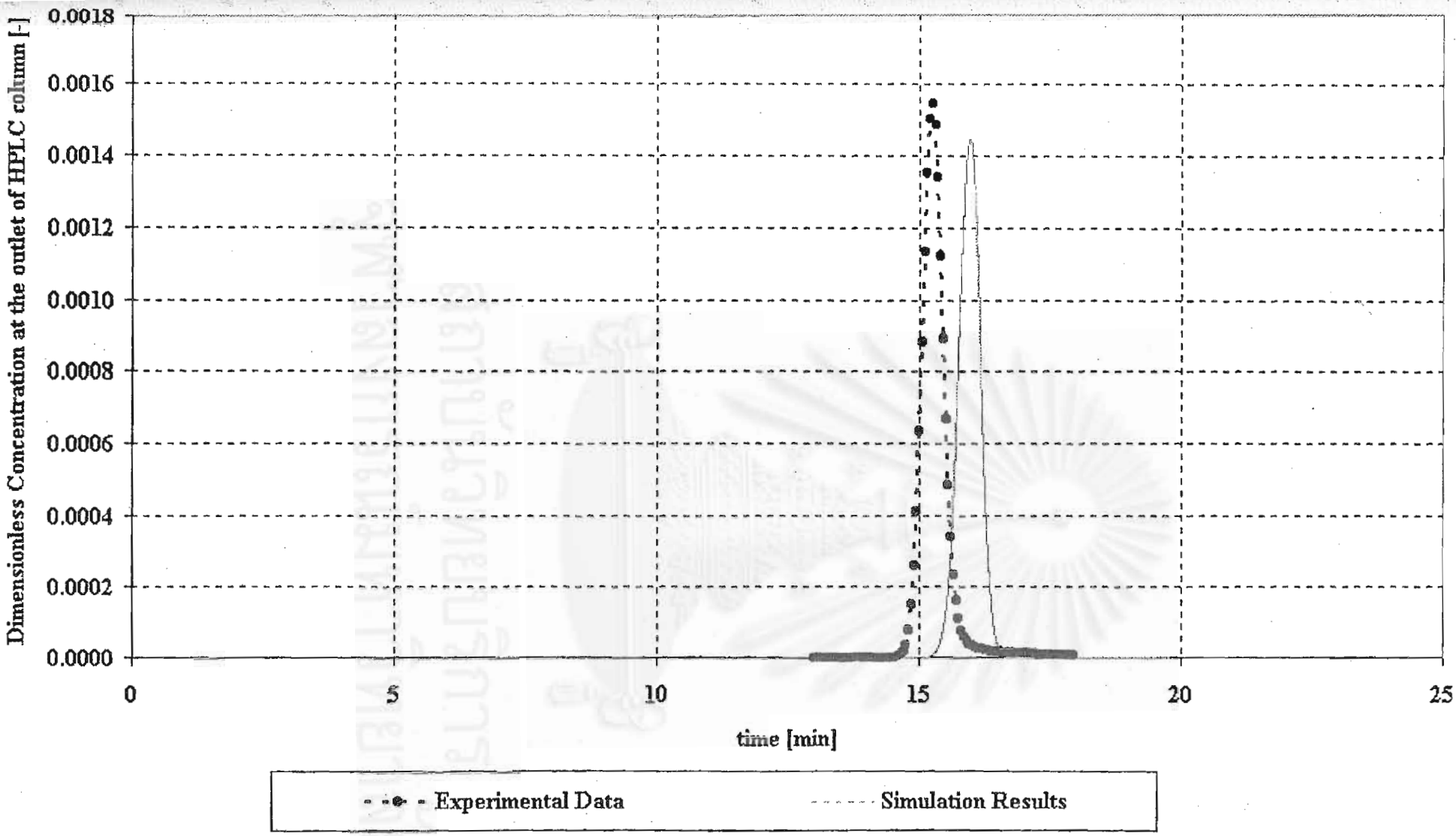

Figure 6.4.1 Comparison between the experimental data and the simulation results of daidzin 0.072 mg/ml at flow rate 1.0 ml/min, St = 32,000, ee = 0.3508, ep = 0.2583, K = 5.1015

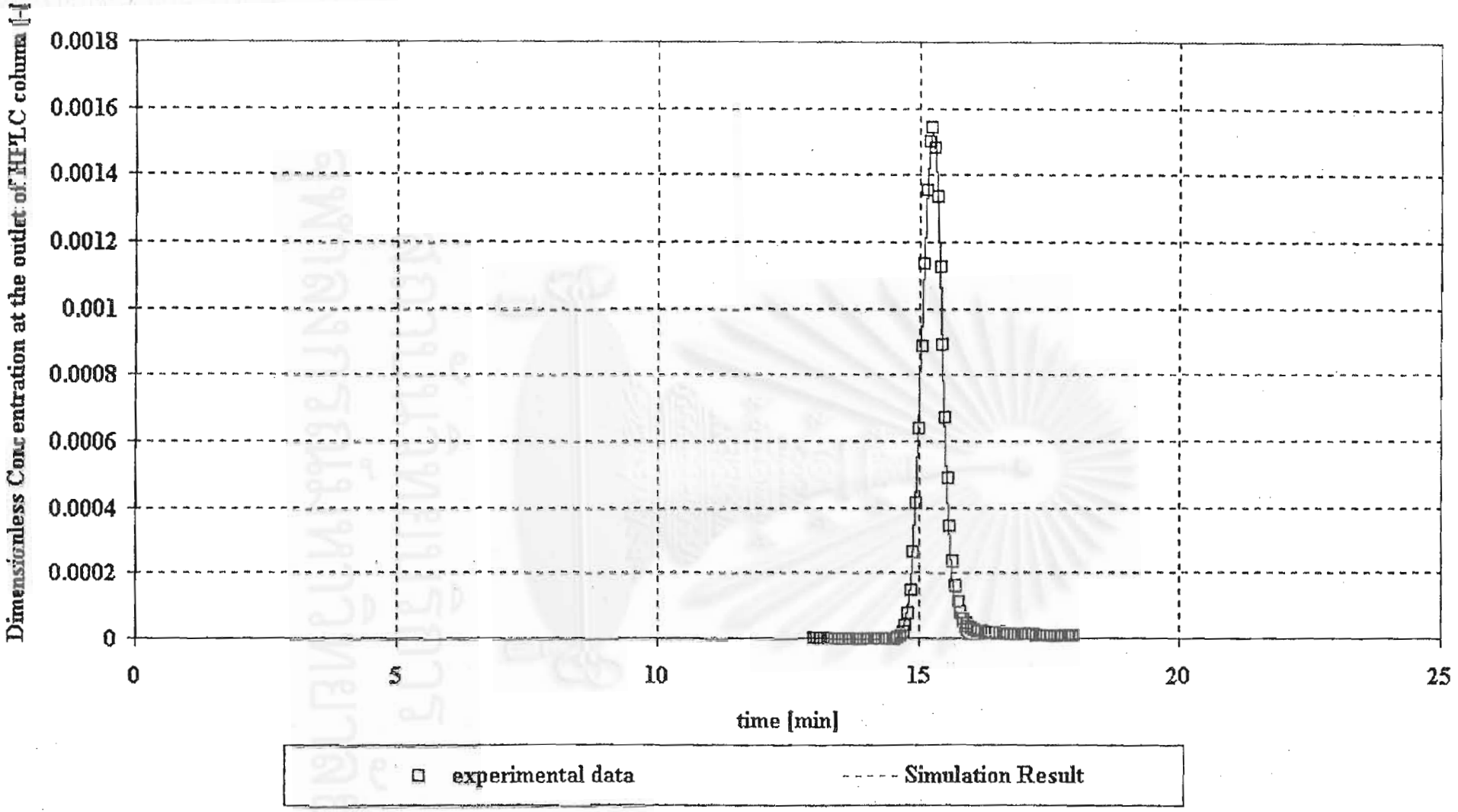

Figure 6.4.2 Comparison between the experimental data and the simulation results of daidzin 0.072 mg/ml at flow rate 1.0 ml/min, St = 32,000, ee = 0.3508, ep = 0.05, K = 5.3098

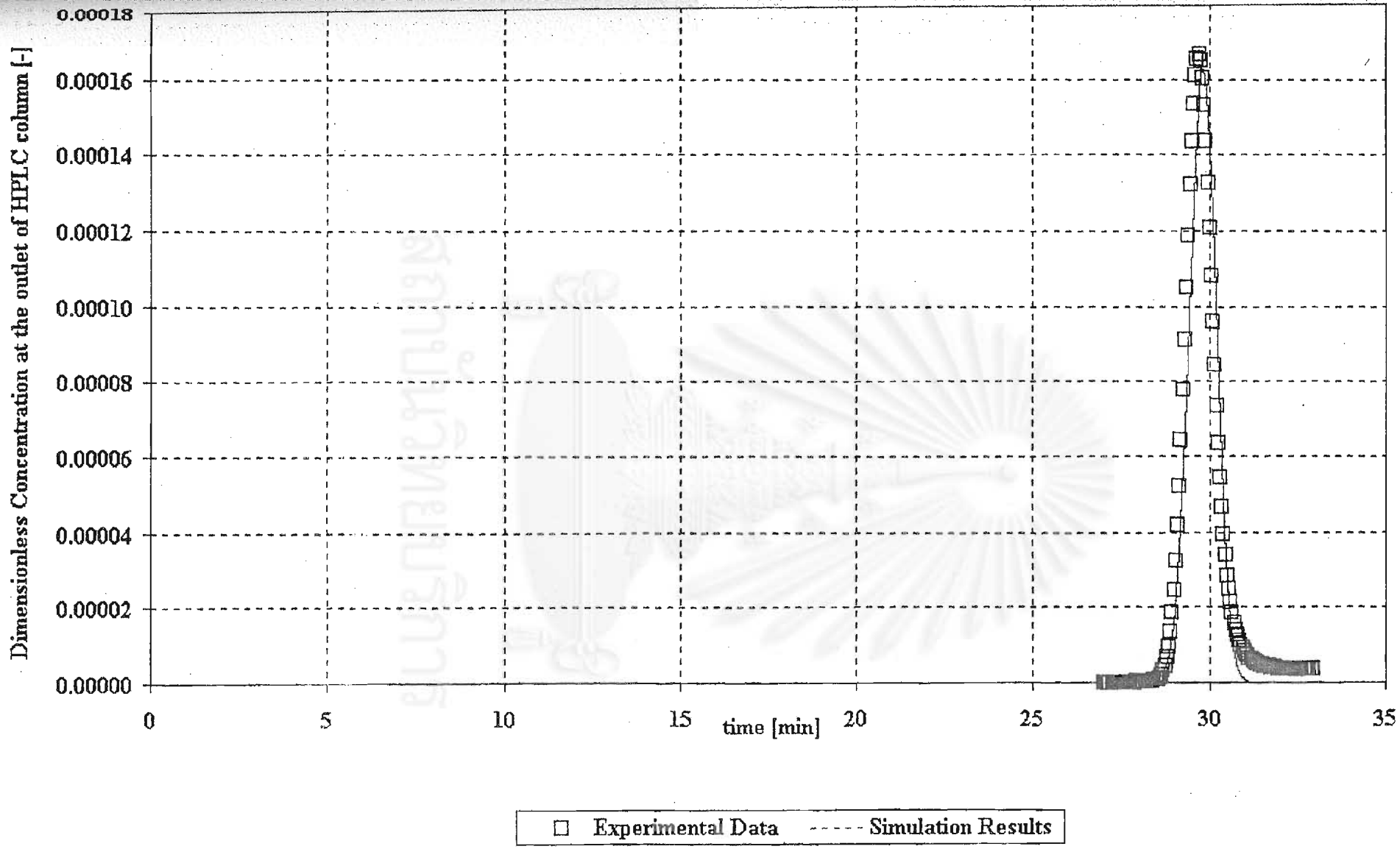

Figure 6.4.3 Comparison between the experimental data and the simulation results of genistin 0.016 mg/ml at flow rate 1.0 ml/min, St = 35,000, ee = 0.3508, ep = 0.05, K = 10.1198

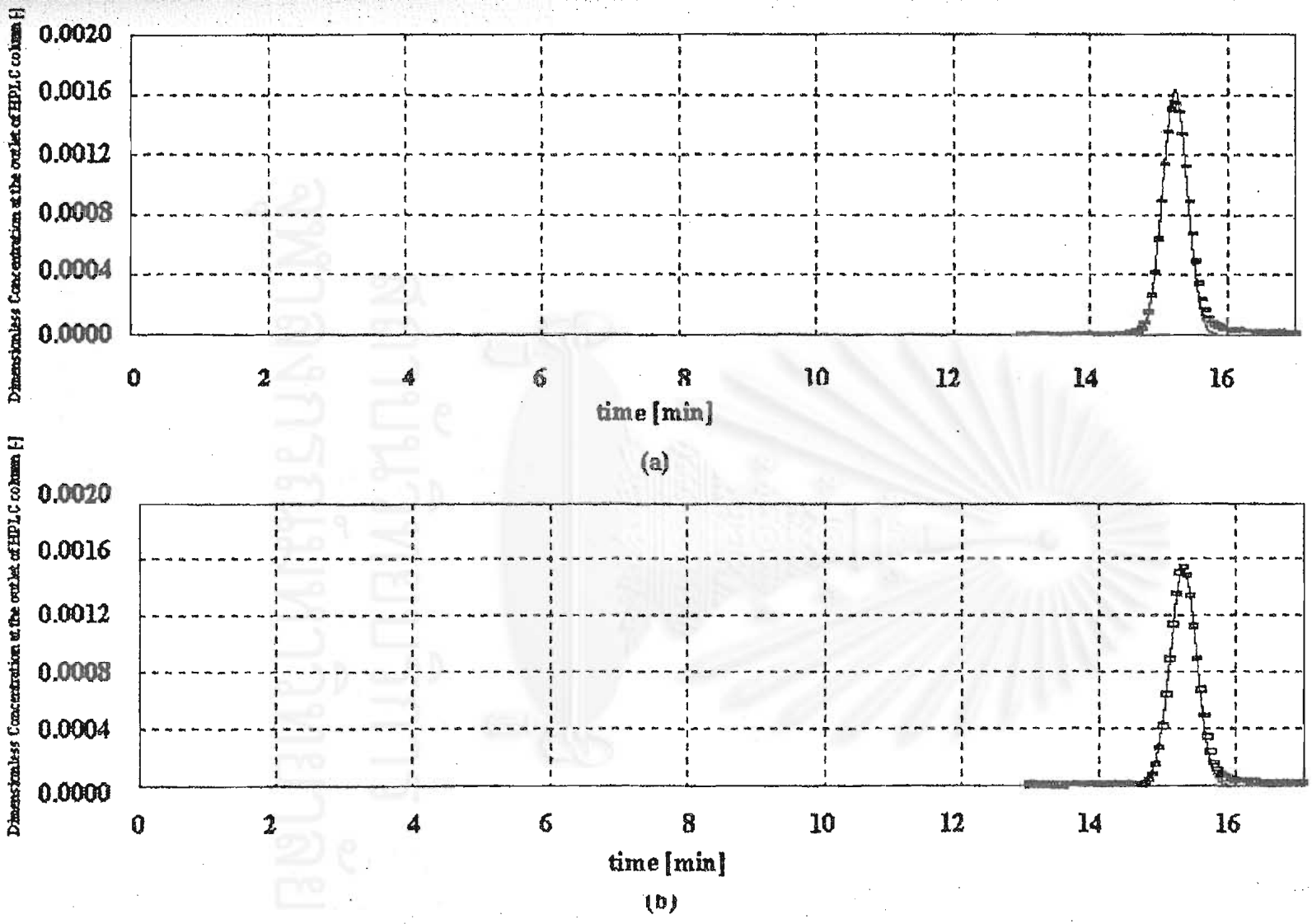

Figure 6.5.1 Comparison between the experimental data (□) and the simulation results (--) of daidzin 0.072 mg/ml at flow rate 1.0 ml/min, St = 32,000, ee = 0.3508, ep = 0.05, K = 5.3098
(a) simulation with axial dispersion term, (b) simulation without axial dispersion term

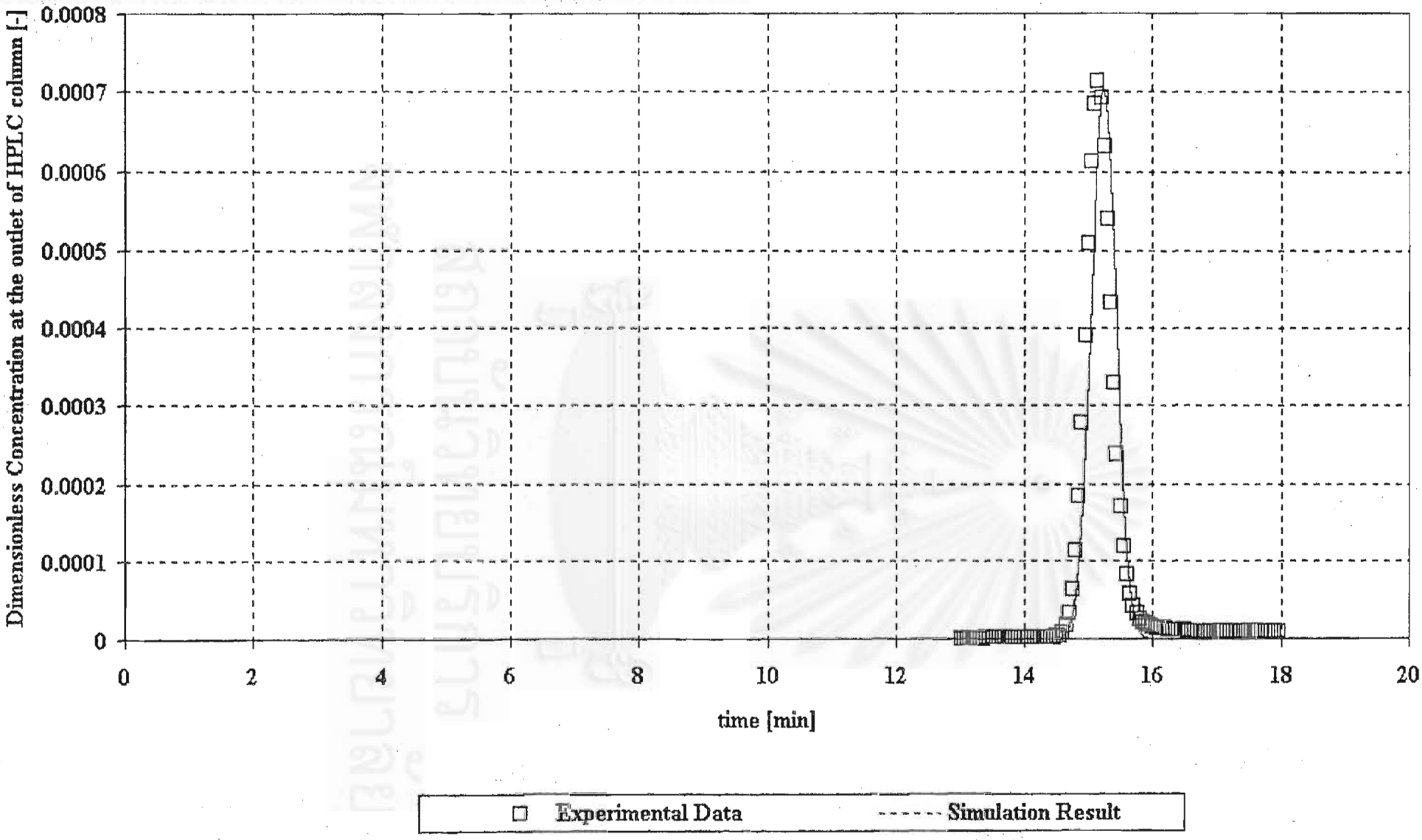

Figure 6.7.1 Comparison between the experimental data and the simulation results of daidzin 0.036 mg/ml at flow rate 1.0 ml/min, St = 32.000, ee = 0.3508, ep = 0.05, K = 5.3098

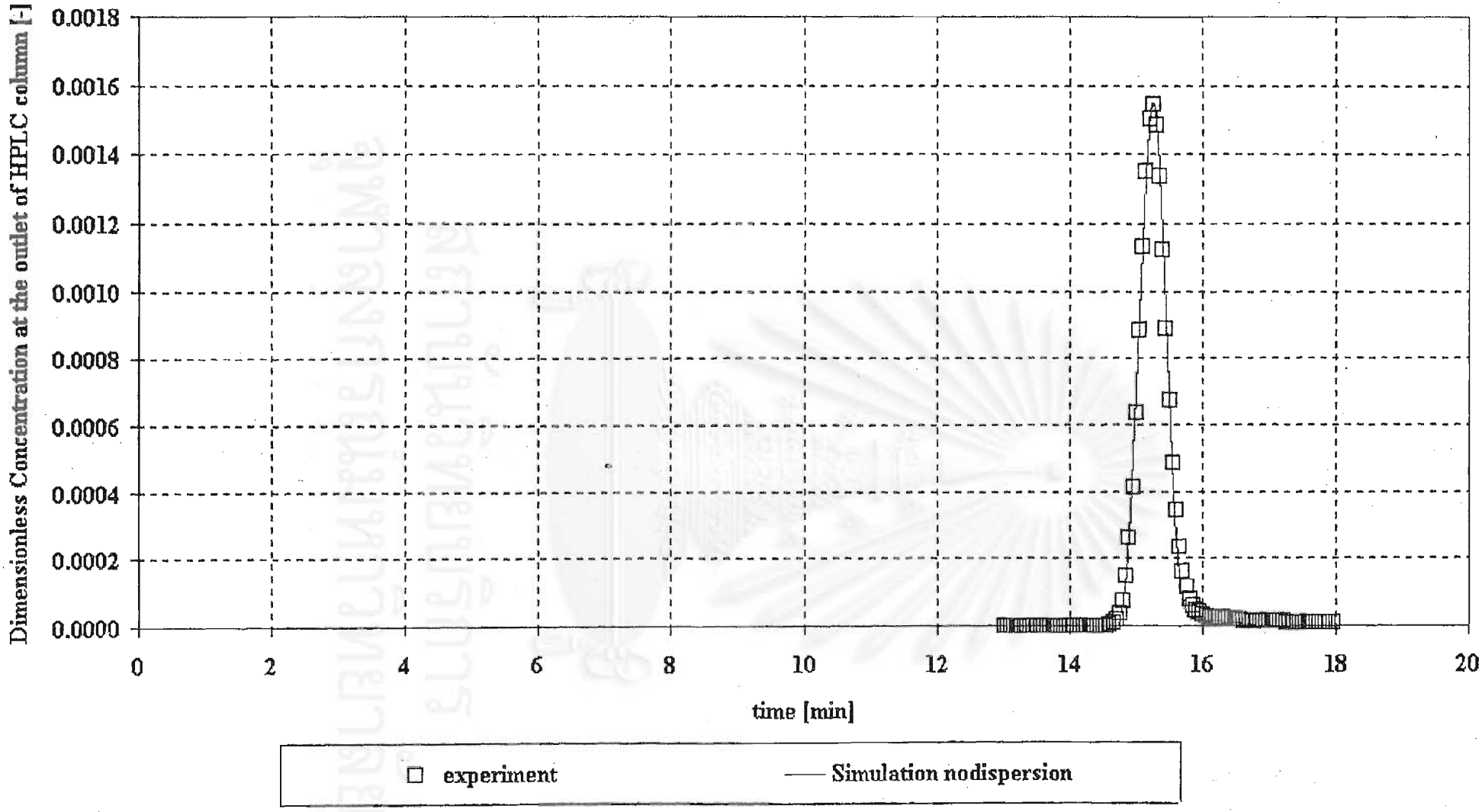

Figure 6.7.2 Comparison between the experimental data and the simulation results of daidzin 0.072 mg/ml at flow rate 1.0 ml/min, St = 32,000, ee = 0.3508, ep = 0.05, K = 5.3098

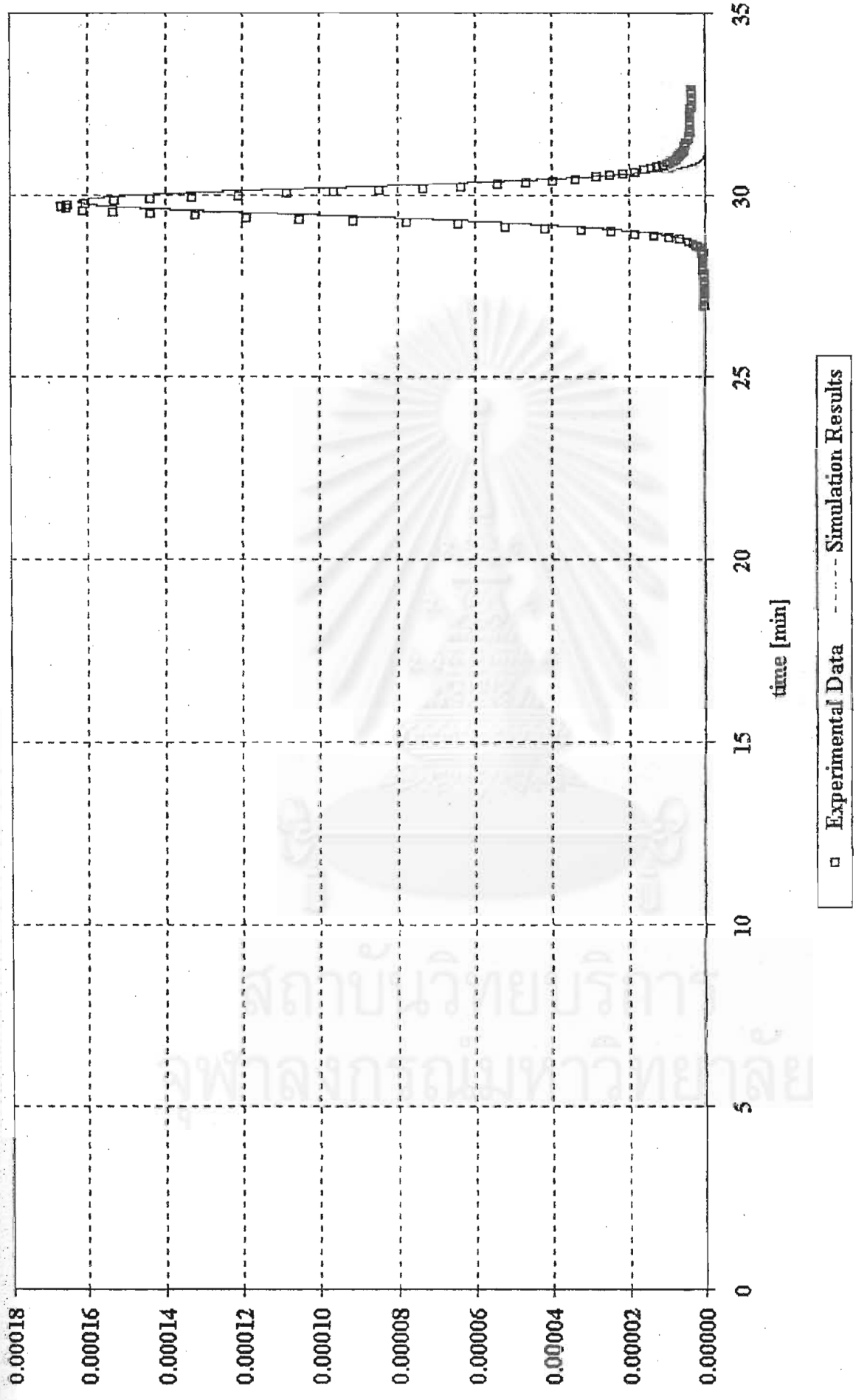

Figure 6.7.3 Comparison between the experimental data and the simulation results of genistin 0.016 mg/ml at flow rate 1.0 ml/min, St = 35,000, ee = 0.3508, ep = 0.05, K = 10.1198

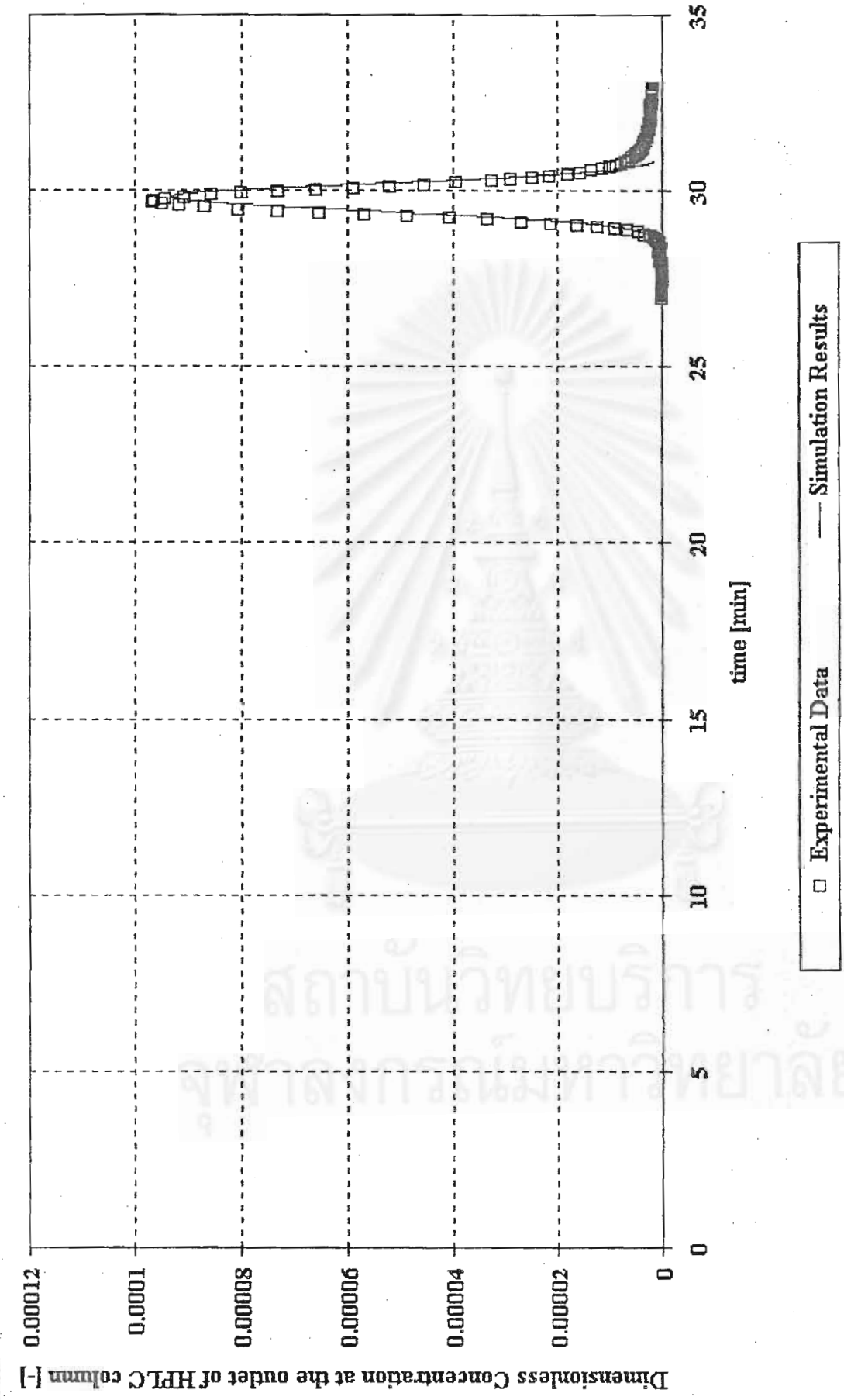

Figure 6.7.4 Comparison between the experimental data and the simulation results of genistin 0.008 mg/ml at flow rate 1 ml/min
St 35000 ee = 0.3508, ep = 0.05 K = 10.1198

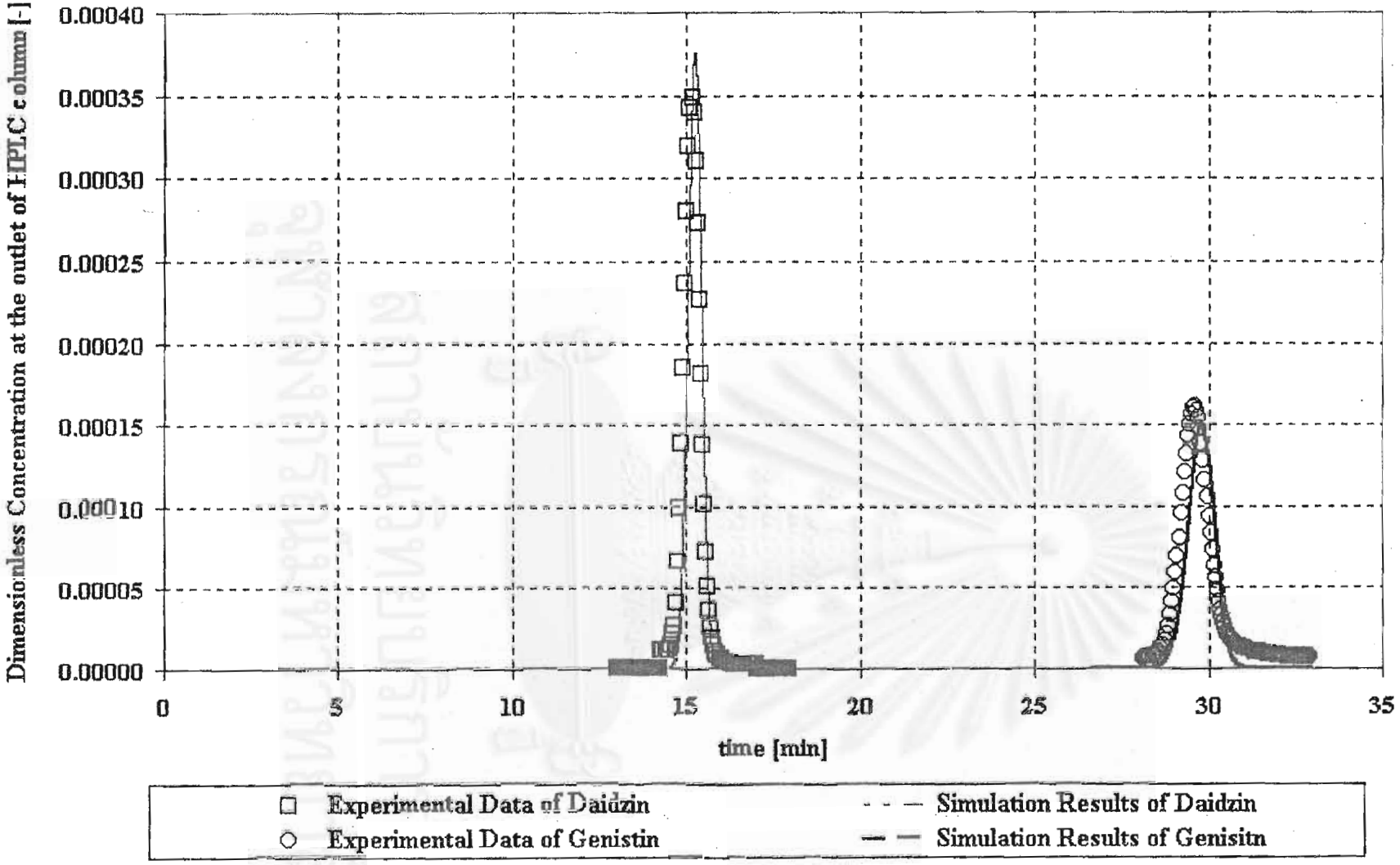

Figure 6.7.5 Comparison between the experimental data and the simulation results of soydilute20 at flow rate 1.0 ml/min, St = 32,000 (daidzin), St = 35,000 (genistin), ee = 0.3508, ep = 0.05, K = 5.3098 (daidzin), K = 10.9951(genistin)

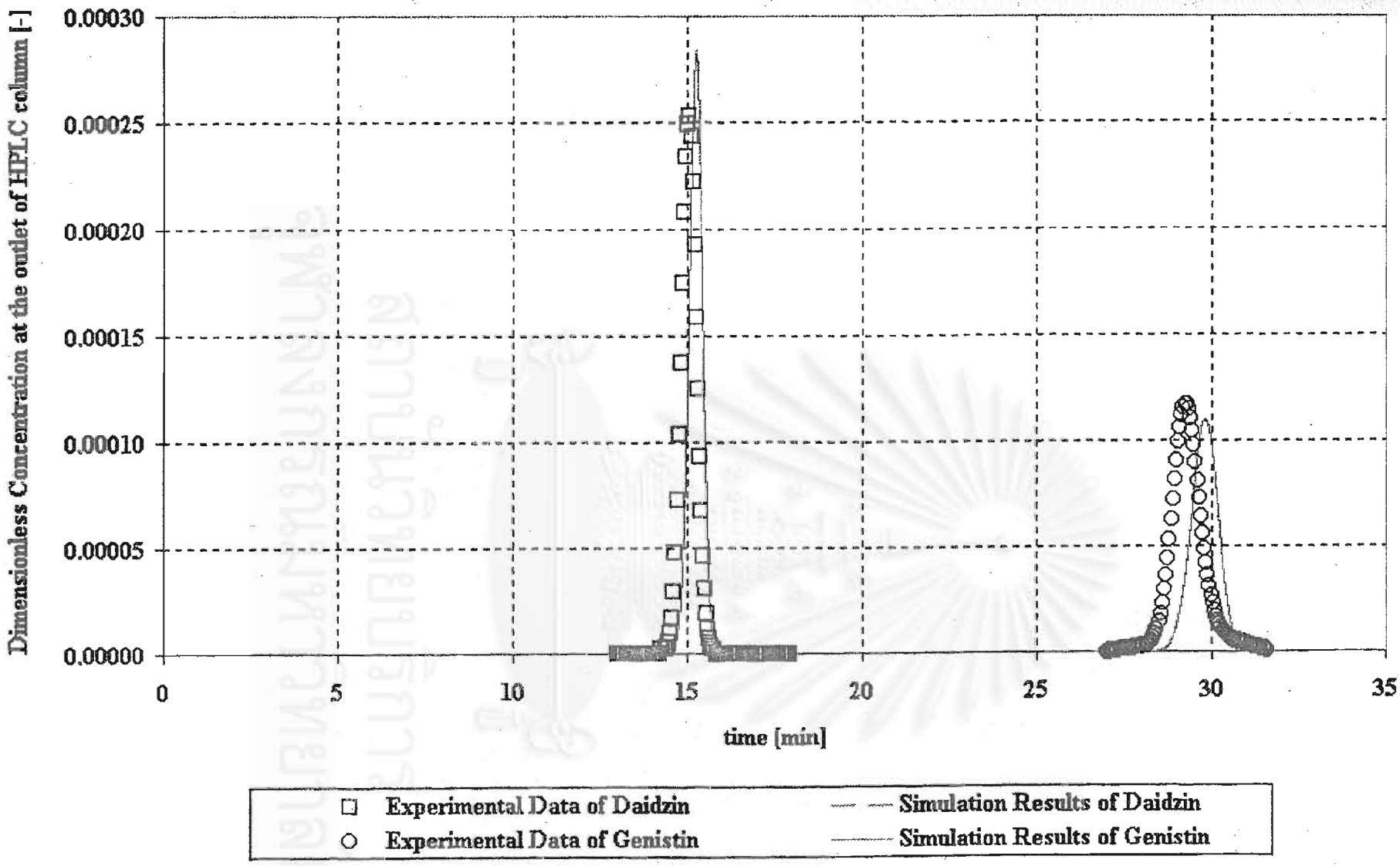

Figure 6.7.6 Comparison between the experimental data and the simulation results of soydilute25 at flow rate 1.0 ml/min, St = 32,000 (daidzin), St = 35000 (genistin), ee = 0.3508, ep = 0.05, K = 5.3098 (daidzin), K = 10.9951(genistin)

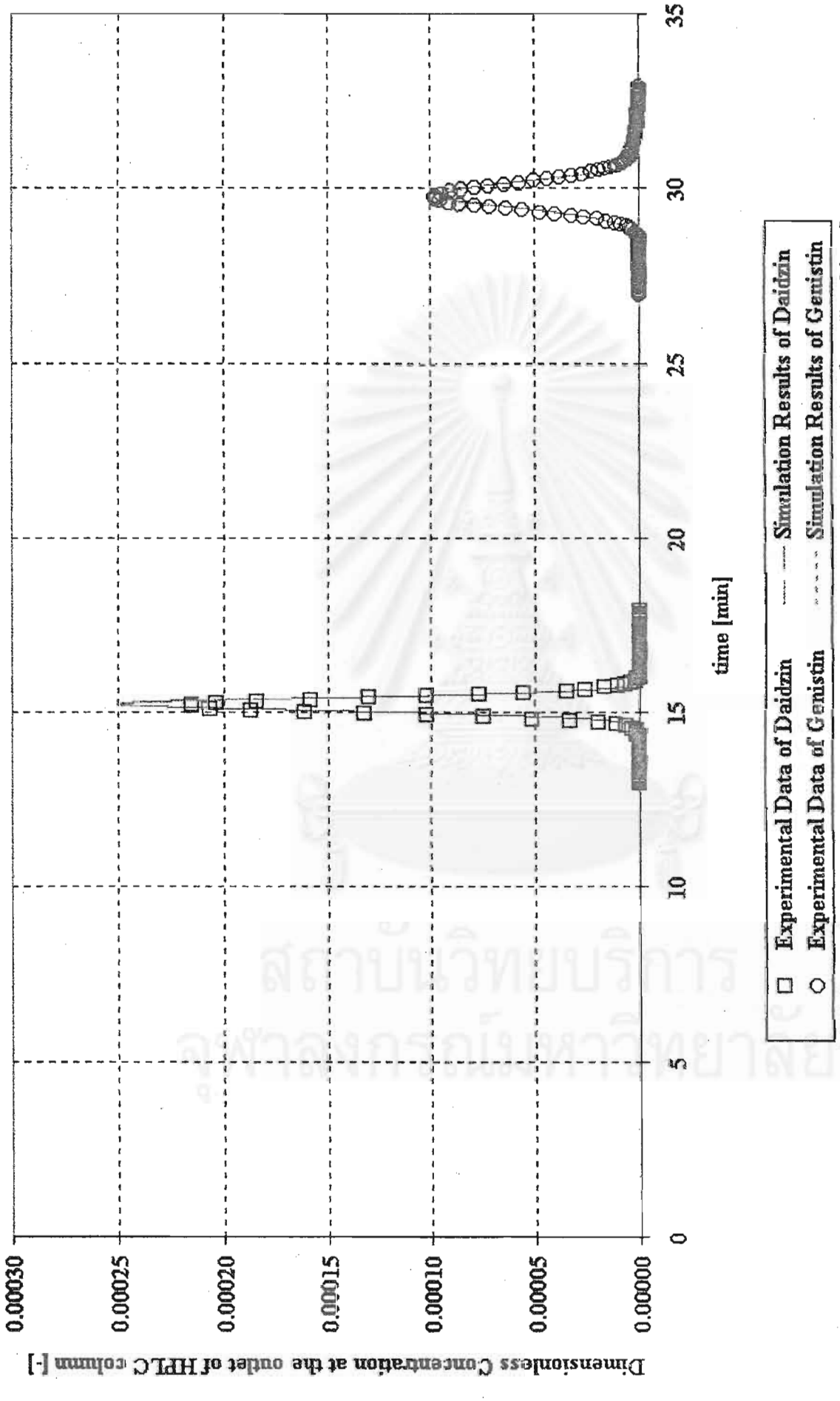

Figure 6.7.7 Comparison between the experimental data and the simulation results of soydilute30 at flow rate 1.0 ml/min, St = 32,000 (daidzin), St = 35000 (genistin), ee = 0.3508, ep = 0.05, K = 5.3098 (daidzin), K = 10.9951 (genistin)

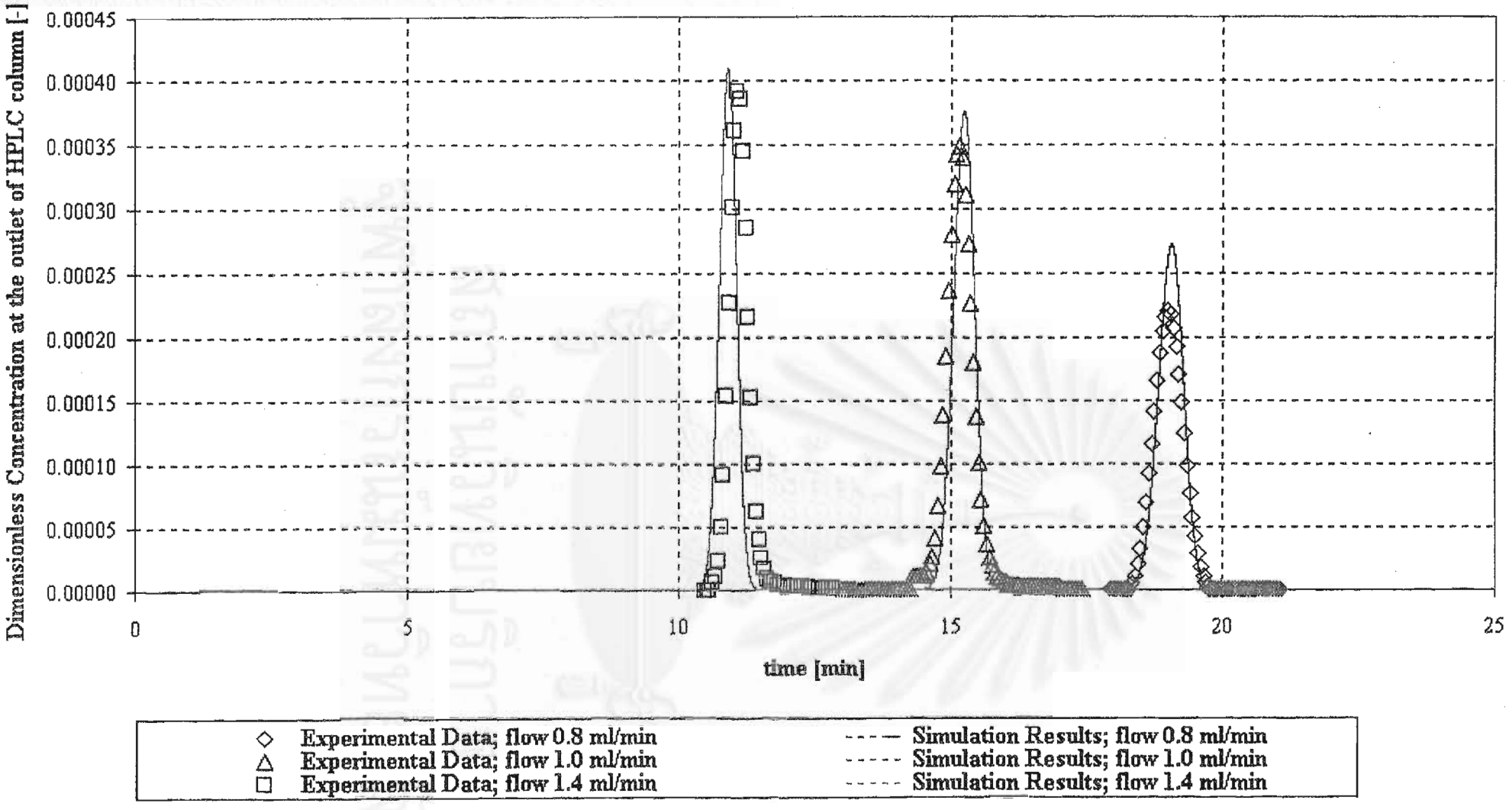

Figure 6.8.1 Comparsion between the experimental data and the simulation results of daidzin 0.012 mg/ml at various flow rate; 0.8 ml/min, 1.0 ml/min, 1.4 ml/min

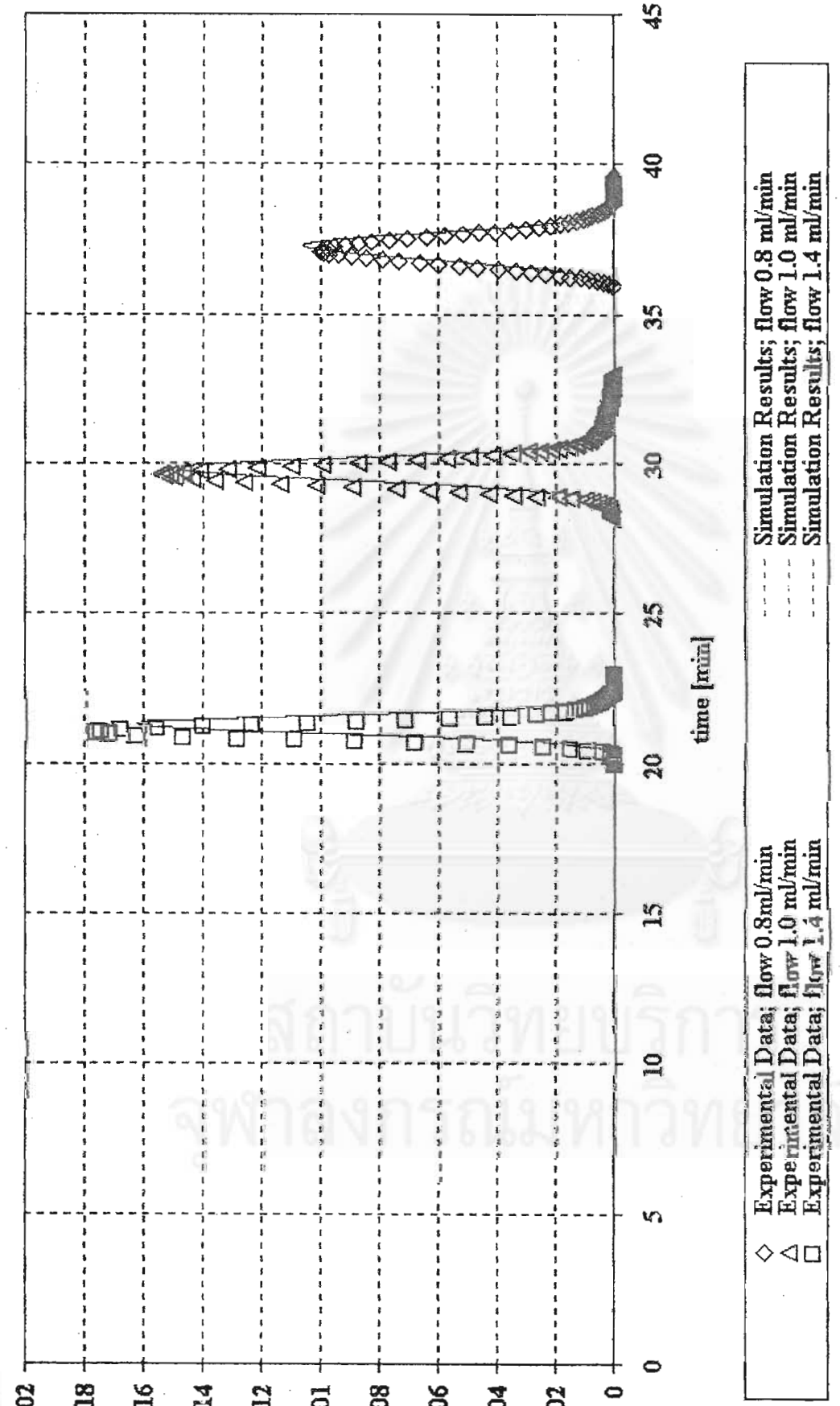

Figure 6.3.2 Comparison between the experimental data and the simulation results of genistin 0.014 mg/ml at various flow rate; 0.8 ml/min, 1.0 ml/min, 1.4 ml/min

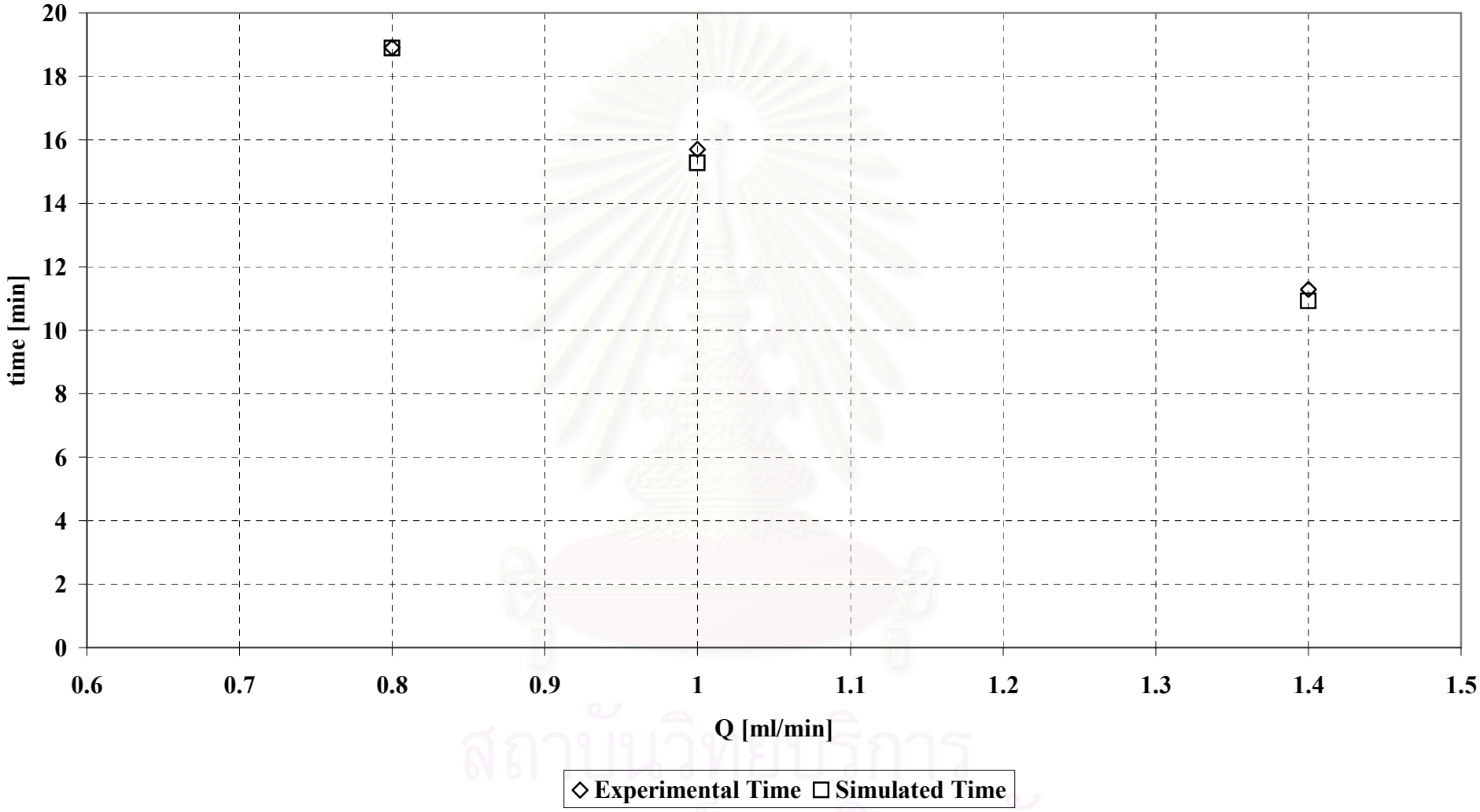

Figure 6.8.3 The comparison resident time of daidzin between experiment and simulation at various flow rate

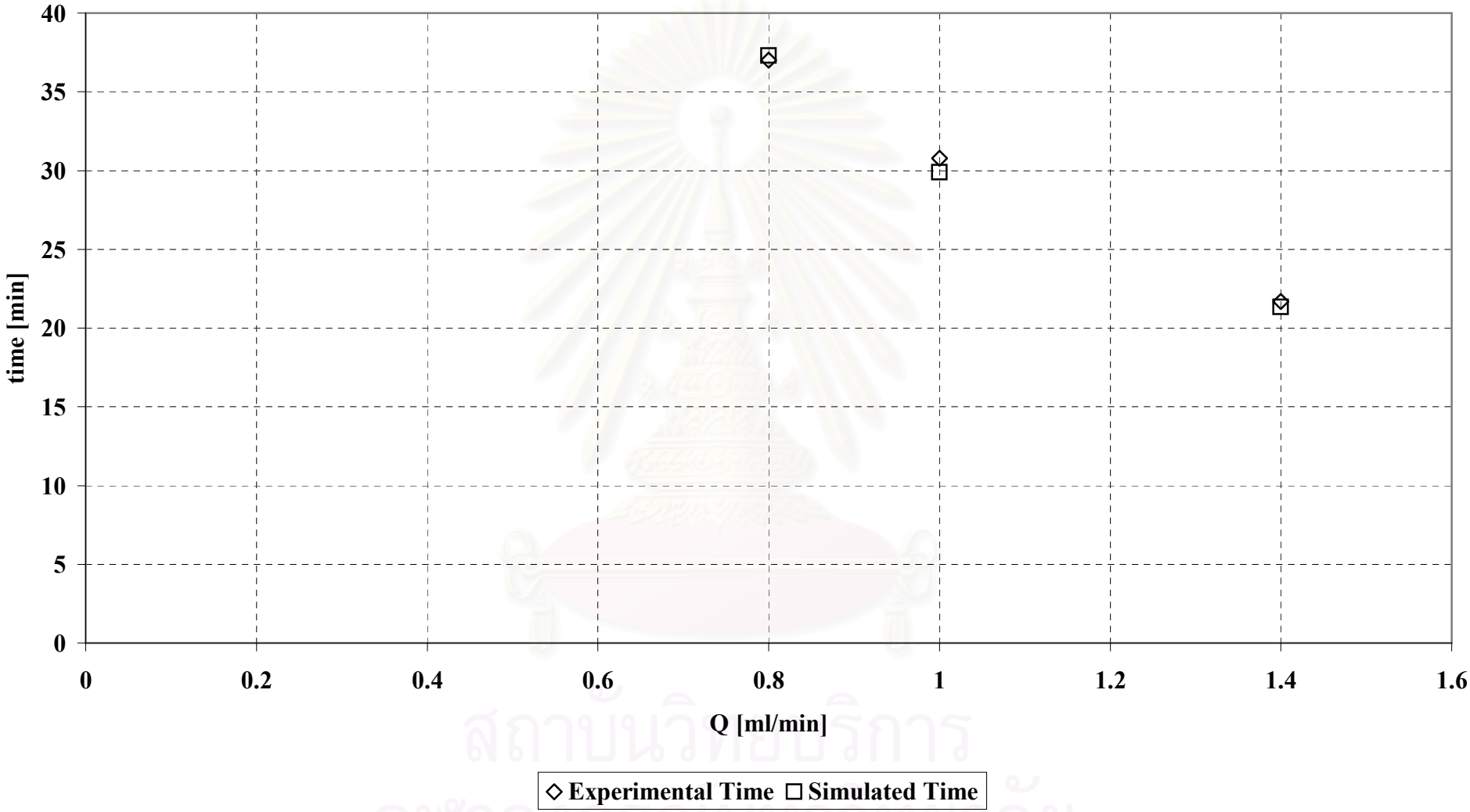

Figure 6.8.4 The comparison resident time of daidzin between experiment and simulation at various flow rate

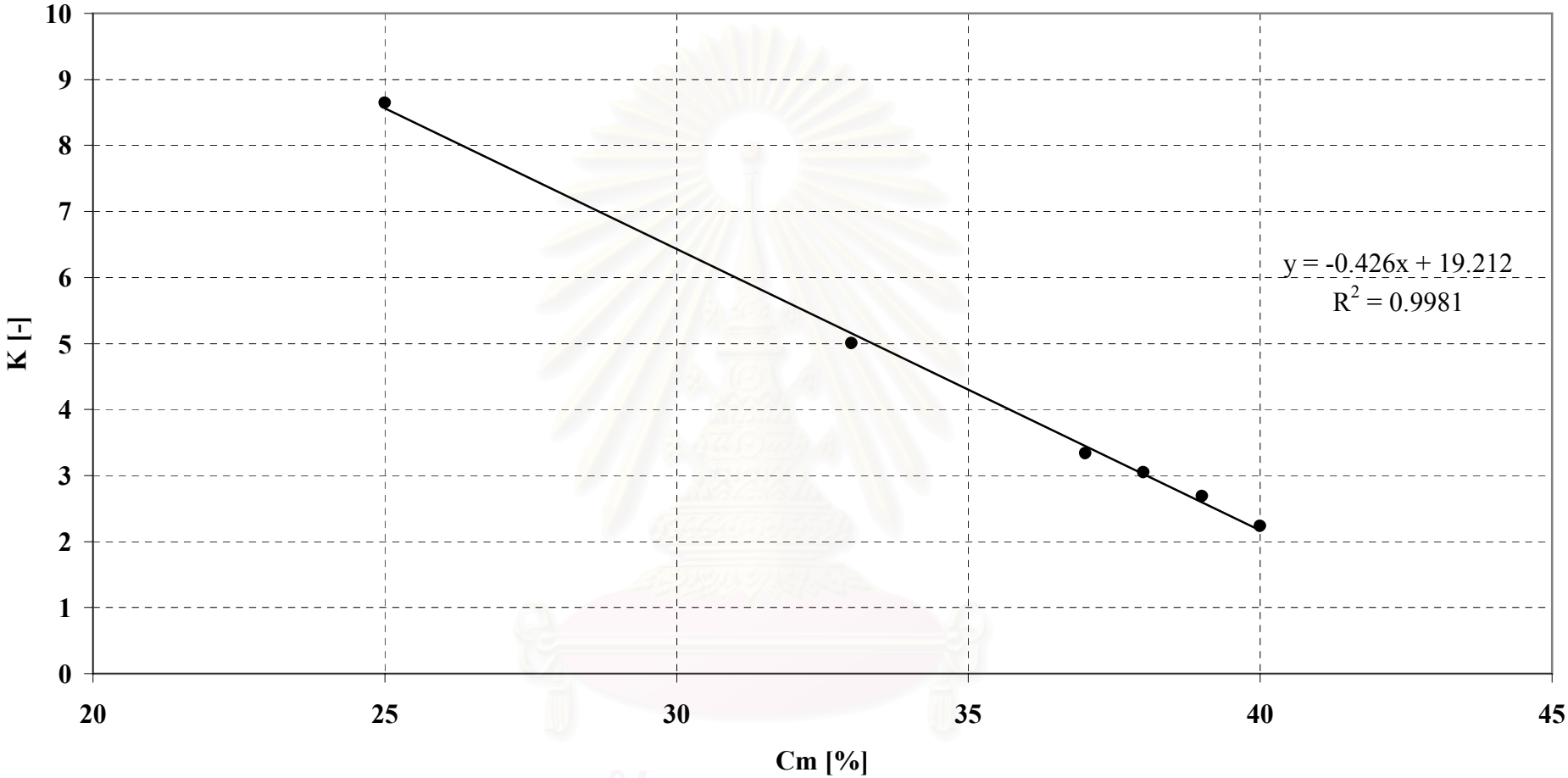

Figure 6.9.1 Adsorption equilibrium of daidzin versus concentration of mobile phase

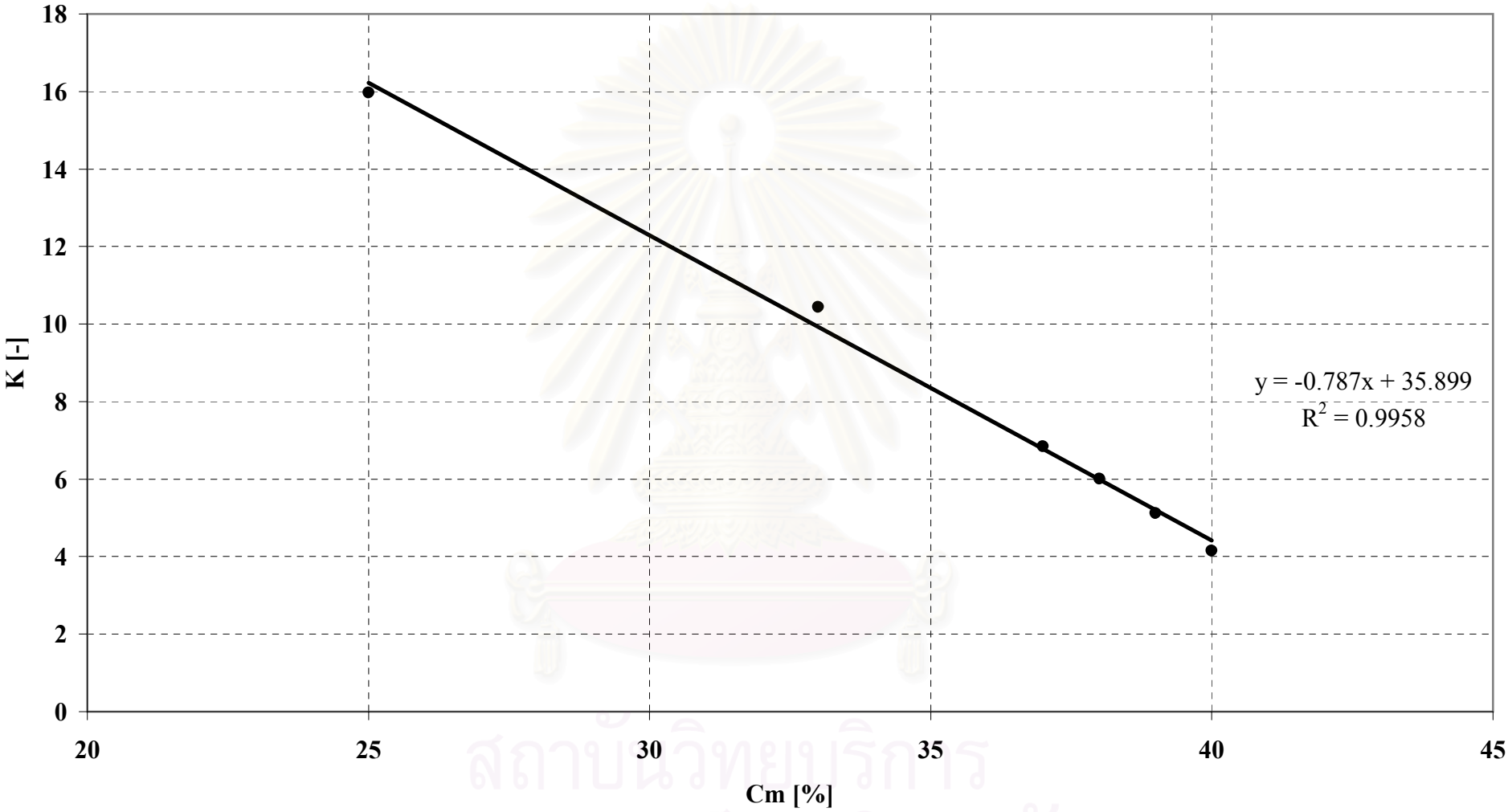

Figure 6.9.2 Adsorption equilibrium of genistin versus concentration of mobile phase

CHAPTER 7

Conclusions and Recommendations

7.1 Mobile Phase for the Separation

Among acetonitrile-water, ethanol-water, and methanol-water, methanol-water is selected to be the most suitable mobile phase in the HPLC system of our study. The optimum concentration of methanol for the separation of daidzin and genistin from the other components in soybean flake extracts with the minimum run time is 33% aqueous solution.

7.2 Revision of the Internal Porosity and the Adsorption Equilibrium Constant

The value of internal porosity estimated from BET and Pore Sizer can not be used in the simulation because the size of daidzin and genistin molecules is in the range of the pore size diameter of the packing. Therefore, almost of daidzin and genistin molecules can not diffuse into the pore of the packing. Hence the value of the internal porosity term has to be revised by trial and error. After that, the adsorption equilibrium to apply for the simulation is estimated from the revised internal porosity. Simulation results using the revised internal porosity and the revised adsorption equilibrium agree well with the experimental data.

7.3 Comparison between Simulation Program with Axial Dispersion Term and without Axial Dispersion Term

Axial dispersion coefficient for this system is very small (4.3E-8 m^2/s) so the simulation without the axial dispersion term can be the same as the simulation with the axial dispersion term. Moreover, times of calculation using the simulation without the

axial dispersion term are 8-9 times faster (480 minutes) than the simulation with the axial dispersion term (4680 minutes).

7.4 Estimation of the Mass Transfer Coefficient

The mass transfer coefficient is affected from the flow rate of mobile phase. For this study, first, the mass transfer coefficient at 1 ml/min of the mobile phase was estimated by trial and error. After that, the correlation by Wilson and Geankoplis, 1966 ($k\alpha\ Re^{0.33}$) was used to estimate the mass transfer coefficient at other flow rates based on the mass transfer coefficient value at flow rate of 1 ml/min.

7.5 Effect of the Injected Sample Concentration on the Simulation

The simulation can predict the separation of daidzin and genistin in the HPLC system when the injected concentration of standard samples is changed. The simulation can still predict well even if the samples are from soybean flake extract solution. Because of the dilution in the HPLC system, other components in the extract solution do not affect to daidzin and genistin separation. However, small errors from the prediction of the resident time and the peak height were observed in some samples.

7.6 Effect of the Flow Rate of the Mobile Phase on the Simulation

The simulation can well predict the isoflavone separation in HPLC system when the flow rate of the mobile phase is changed. From the results, increasing flow rate of the mobile phase reduced the elution time. The estimated mass transfer coefficient from the correlation by Wilson and Geankoplis (1966) can be used to predict the separation of daidzin and genistin.

7.7 Determination of the Relationship between the Concentration of Mobile Phase and the Adsorption Equilibrium of Daidzin and Genistin

Composition of mobile phase affects the adsorption equilibrium constant, therefore affects the elution time of each components. The relationship between the concentration of methanol in the mobile phase and the adsorption equilibrium is useful for the determination of the optimum gradient concentration. For the isoflavone separation, in this study, the relationship between the concentration of methanol in the mobile phase and the adsorption equilibrium is found to be linear.

7.8 Recommendations

The simulation of isoflavone separation in this study can be further applied in a larger HPLC column but the radial dispersion should be considered. Application of the gradient elution can reduce the retention time of isoflavone separation. The relationship between the concentration of methanol in the mobile phase and the adsorption equilibrium of daidzin and genistin as shown in the section 6.9 in the chapter 6 is the useful data for developing the separation by using the gradient method.

REFERENCE

Anderson, J. W., Johnstone, B. M., and Cook-Newell, M. E. 1995. Meta-analysis of the effects of soy protein intake on serum lipids. **The New England Journal of Medicine** 333: 276-282.

Anthony, M. S., Clarkson, T. B., Hughes, JR., C. L., Morgan, T. M., and Burke, G. L. 1996. Soybean isoflavones improve cardiovascular risk factors without affecting the reproductive system of peripubertal rhesus monkeys. **Journal of Nutrition** 126: 43-50.

Arjmandi, B. H., Alekel, L., Hollis, B. W., Amin, D., Stacewicz-sapuntzakis, M., Guo, P., and Kukreja, S. C. 1996. Dietary soybean protein prevents bone loss in an ovariectomized rat model of osteoporosis. **Journal of Nutrition** 126: 161-167.

Barnes, S., Kirk, M., and Coward, L. 1994. Isoflavones and their conjugates in soy foods: extraction conditions and analysis by HPLC-mass spectrometry. **Journal of Agricultural & Food Chemistry** 42: 2466-2474.

Berninger, J. A., Whitley, R. D., Zhang, X., and Wang, N. –H. L. 1991. A versatile model for simulation of reaction and nonequilibrium dynamics in multicomponent fixed-bed adsorption processes. **Computers & Chemical Engineer** 15(11): 749-768.

Carlson, R. E., and Dolphin D. 1978. High-performance liquid chromatographic method for the analysis of isoflavone**. Journal of Chromatography** 198: 193-197.

Carlson, R. E., and Dolphin, D. 1980. High-performance liquid chromatographic method for the analysis of isoflavones. **Journal of Chromatography** 198: 193-197.

Choi, Y. S., and Row, K. H. 2000. Preparative separation of isoflavones from soybean by reversed-phase high performance liquid chromatography**. Journal of Liquid Chromatography & Related Technologies** 23:(11) 1671-1679.

Chung, S. F., and Wen, C. Y. 1968. Longitudinal dispersion of liquid flowing through fixed and fluidized beds. **AIChE Journal** 14: 857-866.

Coward, L., Barnes, N. C., Setchell, KDR., and Barnes, S. 1993. Genistein, daidzein, and their β-glycoside conjugates: antitumor isoflavones in soybean foods from american and asian diets. **Journal of Agriculture and Food Science** 41: 1961-1967.

Czok, M., and Guiochon, G. 1990a. Comparison of the results obtained with different models for the simulation of preparative chromatography. **Computers & Chemical Engineer** 14(2): 1435-1443.

Czok, M., and Guiochon, G. 1990b. The physical sense of simulation models of liquid chromatography: propagation through a grid or solution of the mass balance equation?. **Analytical Chemistry** 62: 189-200.

Dran, H. M., Patterson, D. S. P., Roberts B. A., and Saba, N. 1979. Oestrogenic activity of soya-bean products. **Food and Cosmetics Toxicology** 18: 425-427.

Eldridge, A. C. 1982. High-performance liquid chromatography separation of soybean isoflavones and their glucosides. **Journal of Chromatography** 234: 494-496.

Farmakalidis, E., and Murphy P. A. 1985. Isolation of 6"-O-Acetylgenistin and 6"-O-Acetyldaidzin from toasted defatted soyflakes. **Journal of Agricultural & Food Chemistry** 33: 385-389.

Fukutake, M., Takahashi, M., Ishida, K., Kawamura, H., Sugimura, T., and Wakabayashi, K. 1996. Quantification of genistein and genistin in soybeans and soybean products. **Food and Chemical Toxicology** 34(5): 457-461.

Gugger, Eric, T., Dueppen, and Daniel, G. 1997. Production of isoflavone enriched fractions from soy protein extracts. **U.S. Patent** No. 5,702,752.

Hui, E., Henning, S. M., Park, N., Heber, D., and Go, V. L. W. 2001. Genistein and daidzein/glycitein content in tofu. **Journal of Food Composition and Analysis** 14: 199-206.

Hutabarat, L. S., Mulholland, M., and Greenfield, H. 1998. Development and validation of an isocratic high-performance liquid chromatographic method for quantitative determination of phytoestrogens in soya bean. **Journal of Chromatography A** 795(2): 377-382

Hutabarat, L. S., Greenfield, H., and Mulholland, M. 2001. Isoflavones and coumestrol in soybeans and soybean products from Australia and Indonesia. **Journal of Food Composition and Analysis** 14: 43-58.

Kaczmarki, K. 1996. Use of orthogonal collocation on finite elements with moving boundaries in the simulation of non-linear multicomponent chromatography. Influence of fluid velocity variation on retention time in LC and HPLC. **Computers & Chemical Engineer** 20(1): 49-64.

Ma, Z., and Guichon, G. 1991. Application of orthogonal collocation on finite-elements in the simulation of non-linear chromatography. **Computers & Chemical Engineer** 15(6): 415-426.

Messina, M., and Barnes, S. 1991. Commentary: The role of soy products in reducing risk of cancer. **Journal of the National Cancer Institute** 83(8): 541-546.

Miksicek, RJ. 1995. Estrogenic flavonoids: structural requirements for biological activity. **Proceedings of the Society for Experimental Biology and Medicine** 208: 44-50.

Murphy, P. A. 1981. Separation of genistin, daidzin and their aglucones, and coumesterol by gradient high-performance liquid chromatography. **Journal of Chromatography** 211: 166-169.

Murphy, P. A. 1982. Phytoestrogen content of processed soybean products. **Food Technology** 36: 60-64.

Park, Y. K., Row, K. H., and Chung, S. T. 2000. Adsorption characteristics and separation of taxol from yew tree by NP-HPLC. **Separation and Purification Technology** 19: 27-37.

Peterson, G., and Barnes, S. 1991. Genistein inhibition of the growth of human breast cancer cells: independence from estrogen receptors and the multi-drug resistance gene. **Biochemical and Biophysical Research Communications** 179(1): 661-667.

Pratt, D. E.,and Birac, P. M. 1979. Source of antioxidant of soybeans and soy products. **Journal of Food Science** 44: 1720-1722.

Rouchon P., Schonauer, M., Valentin, P., and Guiochon, G. 1987. Numerical simulation of band propagation in nonlinear chromatography. **Separation Science and Technology** 22: 1793.

Sereno, C., Rodrigues, Villadsen, J. 1991. The moving finite element method with polynomial approximation of any degree. **Computers & Chemical Engineer** 15(1): 25-33.

Sereno, C., Rodrigues, A., and Villadsen, J. 1992. Solution of partial differential equations systems by the moving finite element method. **Computers & Chemical Engineer** 16(6): 583-592.

Setchell, KDR., Lawson, A. M., Borrielo, S. P., Harkness, R., Gordon, H., Morgan, DML., Kirk, D. N., Adlercreutz, H., Anderson, L. C., and Axelson, M. 1981. Lignan formation in man. **Lancet** i: 4-7.

Setchell, KDR., and Adlercrueutz, H. 1988. Mammalian lignans and phytoestrogens. **In the role of the gut flora in toxicity and cancer** pp. 315-346. Academic Press, London.

Setchell, KDR., Borriello, SP., Hulme, P., Kirk, DN., and Axelson, M. 1984. Nonsteroidal estrogens of dietary origin: possible roles in hormone-dependent disease. **The American Journal of Clinical Nutrition** 40: 569-578.

Shutt, D. A., and Cox, R. I. 1972. Steroid and phytoestrogen binding to sheep uterine receptors *in vivo*. **Journal of Endocrinology** 52: 299-310.

Song, T., Barua, K., Buseman, G., and Murphy P. A. 1998. Soy isoflavone analysis: quality control and a new internal standard. **American Journal of Clinical Nutrition** 68(suppl): 1474S-9S.

Tang, B. Y., and Adams, N. R. 1980. Effects of equol on oestrogen receptors and on synthesis on DNA and protein in the immature rat uterus. **Journal of Endocrinology** 85: 291-297.

Wang, G., Kuan, S. S., Francis, O. J., Ware, G. M., and Carman, A. S. 1990. A simplified HPLC method for the determination of phytoestrogens in soybean and its processed products. **Journal of Agricultural & Food Chemistry** 38: 185-190.

Wang, H. J., and Murphy, P. A. 1994. Isoflavone content in commercial soybean foods. **Journal of Agricultural & Food Chemistry** 42: 1666-1673.

Wang, H. J., and Murphy, P. A. 1996. Mass balance study of isoflavones during soybean processing. **Journal of Agricultural & Food Chemistry** 44: 2377-2383.

West, L. G., Birac, P. M., and Pratt, D. E. 1978. Separation of the isomeric isoflavones from soybeans by high-performance liquid chromatography. **Journal of Chromatography** 150: 266-268.

Yu, Q., and Wang, N. –H. L. 1989. Computer simulations of the dynamics of multicomponent ion exchange and adsorption in fixed beds-gradient-directed moving finite element method. **Computers & Chemical Engineer** 13(8): 915-926.

Appendices

Appendix A

Program source codes

This appendix presents all of the main programs used in this work. The following table gives information about what category of each program was used in this work. All programs were written in MATLAB(VERSION 5.3.1)

Program Name	Usage
#1	Mathematical model is not covered with axial dispersion term of the HPLC column
#2	Mathematical model is covered with axial dispersion term of the HPLC column

```
#-------------------------------------------------------------------------#
% File name: #1;
% Finite difference (Explicit, Crank Nicholson) and Range
Kutta;
#-------------------------------------------------------------------------#
clear

%Input characteristic of column
dp   = 5*10^-6; %(equivalent particle diameter [m]);
L    = 0.25; %(column length[m]);
ee   = 0.3508; %(external void fraction);
ep   = 0.05 %(internal void fraction);
Di   = 4.6*10^-3;%(diameter of HPLC column [m]);

%Input condition of experiment
t1   = 1020; %(run time [s] );
tp   = 4; %(time for injection [s]);
Q    = 1;%(flow rate of mobile phase[ml/min]);
Q    = Q/(60*10^6);%(flow rate of mobile phase [m3/sec]);
A    = pi*(Di/2)^2; %(crossectional area of column);
u    = Q/(ee*A); %(interstitial velocity of mobile phase[m/s]);
uf   = 0.0005; %( reference velocity[m/s]);
tal1 = t1*uf/L;%(dimensionless of time, t1);
talp = tp*uf/L;%(dimensionless of time, tp);
yf   = 0.011; %(concentration at the inlet of column);
y0   = 0; %(initial condition1);
yp0  = 0; %(initial condition2);
e    = u/uf;

%Input condition of numerical
deltal = 0.0004;%(step size of time dimensionless);
i      = ceil(tal1/deltal);%(number of interval of time);
delz   = 0.0005;%(step size of distance);
j      = ceil(1/delz); %(number of interval in column);

% Set initial k, l for Runge Kutta term;
k1     =  zeros(j+1,1);
k2     =  zeros(j+1,1);
k3     =  zeros(j+1,1);
k4     =  zeros(j+1,1);
l1     =  zeros(j+1,1);
l2     =  zeros(j+1,1);
l3     =  zeros(j+1,1);
l4     =  zeros(j+1,1);

% Input parameter
K      = 5.3098; %(adsorption equilibrium [-]);
k      =   5.3333*10^-5; %(mass transfer coefficient [m/s]);
ap     = 6/dp; %(external surface of the adsorbent pellet
[m^2/m^3]);
St     =   k*ap*L/uf; %(Stanton number);


%  input initial condition

y   =  zeros(j+1,1); %(initial condition of dimensionless
condition in fluid phase);
yp  =  zeros(j+1,1); %(initial condition of dimensionless
condition in the macropore);
for p =1:j+1
  y(p,1)  = y0;
  yp(p,1) = yp0;
```

```
end
y(1,1) = yf; %(dimensionless concentration at the inlet of
column);

%Calculation of constant;

A = St/(ep+(1-ep)*K);
C = -e/(2*delz);
D = -(1-ee)*St/ee;

%Runge Kutta
% t = 0 to t = tp;
for m = 1:ceil(talp/deltal)

  for n = 2:j
    k1(n) = deltal*(C*(y(n+1,1)-y(n-1,1))+D*(y(n,1)-yp(n,1)));
    l1(n) = deltal*(A*(y(n,1)-yp(n,1)));
  end
  k1(j+1) = deltal*(2*C*(y(j+1,1)-y(j,1))+D*(y(j+1,1)-yp
(j+1,1)));
  l1(j+1) = deltal*(A*(y(j+1,1)-yp(j+1,1)));

  for n = 2:j
    k2(n) = deltal*(C*((y(n+1,1)+k1(n+1)/2)-(y(n-1,1)+k1(n-
1)/2))+D*((y(n,1)+k1(n)/2)-(yp(n,1)+l1(n)/2)));
    l2(n) = deltal*(A*((y(n,1)+k1(n)/2)-(yp(n,1)+l1(n)/2)));
  end
  k2(j+1) = deltal*(2*C*((y(j+1,1)+k1(j+1)/2)-(y(j,1)+k1
(j)/2))+D*((y(j+1,1)+k1(j+1)/2)-(yp(j+1,1)+l1(j+1)/2)));
  l2(j+1) = deltal*(A*((y(j+1,1)+k1(j+1)/2)-(yp(j+1,1)+l1
(j+1)/2)));

  for n = 2:j
    k3(n) = deltal*(C*((y(n+1,1)+k2(n+1)/2)-(y(n-1,1)+k2(n-
1)/2))+D*((y(n,1)+k2(n)/2)-(yp(n,1)+l2(n)/2)));
    l3(n) = deltal*(A*((y(n,1)+k2(n)/2)-(yp(n,1)+l2(n)/2)));
  end
  k3(j+1) = deltal*(2*C*((y(j+1,1)+k2(j+1)/2)-(y(j,1)+k2
(j)/2))+D*((y(j+1,1)+k2(j+1)/2)-(yp(j+1,1)+l2(j+1)/2)));
  l3(j+1) = deltal*(A*((y(j+1,1)+k2(j+1)/2)-(yp(j+1,1)+l2
(j+1)/2)));

  for n = 2:j
    k4(n) = deltal*(C*((y(n+1,1)+k3(n+1))-(y(n-1,1)+k3(n-
1)))+D*((y(n,1)+k3(n))-(yp(n,1)+l3(n))));
    l4(n) = deltal*(A*((y(n,1)+k3(n))-(yp(n,1)+l3(n))));
  end
  k4(j+1) = deltal*(2*C*((y(j+1,1)+k3(j+1))-(y(j,1)+k3
(j)))+D*((y(j+1,1)+k3(j+1))-(yp(j+1,1)+l3(j+1))));
  l4(j+1) = deltal*(A*((y(j+1,1)+k3(j+1))-(yp(j+1,1)+l3
(j+1))));

  y(1,1) = yf;
% Calculation of dimensionless concentration at the next step
of time;

for n = 2:j+1
  y(n,1) = y(n,1)+(k1(n)+2*k2(n)+2*k3(n)+k4(n))/6;
  yp(n,1)= yp(n,1)+(l1(n)+2*l2(n)+2*l3(n)+l4(n))/6;
end
yexit(m+1,1) = y(j+1,1);
```

```
if floor(m/1000)==ceil(m/1000)
  fprintf('m=%f \n',m);
  yexit(m,1)
  y(100,1)
  y(300,1)
  y(500,1)
  y(900,1)

end
end

%Runge Kutta
% At t = tp to t = t1;

y(1,1) = 0;
for m = ceil(talp/deltal)+1:ceil(tal1/deltal)

  for n = 2:j
    k1(n) = deltal*(C*(y(n+1,1)-y(n-1,1))+D*(y(n,1)-yp(n,1)));
    l1(n) = deltal*(A*(y(n,1)-yp(n,1)));
  end
  k1(j+1) = deltal*(2*C*(y(j+1,1)-y(j,1))+D*(y(j+1,1)-yp
(j+1,1)));
  l1(j+1) = deltal*(A*(y(j+1,1)-yp(j+1,1)));

  for n = 2:j
    k2(n) = deltal*(C*((y(n+1,1)+k1(n+1)/2)-(y(n-1,1)+k1(n-
1)/2))+D*((y(n,1)+k1(n)/2)-(yp(n,1)+l1(n)/2)));
    l2(n) = deltal*(A*((y(n,1)+k1(n)/2)-(yp(n,1)+l1(n)/2)));
  end
  k2(j+1) = deltal*(2*C*((y(j+1,1)+k1(j+1)/2)-(y(j,1)+k1
(j)/2))+D*((y(j+1,1)+k1(j+1)/2)-(yp(j+1,1)+l1(j+1)/2)));
  l2(j+1) = deltal*(A*((y(j+1,1)+k1(j+1)/2)-(yp(j+1,1)+l1
(j+1)/2)));

  for n = 2:j
    k3(n) = deltal*(C*((y(n+1,1)+k2(n+1)/2)-(y(n-1,1)+k2(n-
1)/2))+D*((y(n,1)+k2(n)/2)-(yp(n,1)+l2(n)/2)));
    l3(n) = deltal*(A*((y(n,1)+k2(n)/2)-(yp(n,1)+l2(n)/2)));
  end
  k3(j+1) = deltal*(2*C*((y(j+1,1)+k2(j+1)/2)-(y(j,1)+k2
(j)/2))+D*((y(j+1,1)+k2(j+1)/2)-(yp(j+1,1)+l2(j+1)/2)));
  l3(j+1) = deltal*(A*((y(j+1,1)+k2(j+1)/2)-(yp(j+1,1)+l2
(j+1)/2)));

  for n = 2:j
    k4(n) = deltal*(C*((y(n+1,1)+k3(n+1))-(y(n-1,1)+k3(n-
1)))+D*((y(n,1)+k3(n))-(yp(n,1)+l3(n))));
    l4(n) = deltal*(A*((y(n,1)+k3(n))-(yp(n,1)+l3(n))));
  end
  k4(j+1) = deltal*(2*C*((y(j+1,1)+k3(j+1))-(y(j,1)+k3
(j)))+D*((y(j+1,1)+k3(j+1))-(yp(j+1,1)+l3(j+1))));
  l4(j+1) = deltal*(A*((y(j+1,1)+k3(j+1))-(yp(j+1,1)+l3
(j+1))));

  y(1,1) = 0;
% Calculation of dimensionless concentration at the next step
of time;

for n = 2:j+1
  y(n,1) = y(n,1)+(k1(n)+2*k2(n)+2*k3(n)+k4(n))/6;
```

```
   yp(n,1)= yp(n,1)+(l1(n)+2*l2(n)+2*l3(n)+l4(n))/6;
end
yexit(m+1,1) = y(j+1,1);
if floor(m/1000)==ceil(m/1000)
   fprintf('m=%f \n',m);
   yexit(m,1)
   y(100,1)
   y(300,1)
   y(500,1)
   y(900,1)

end
end
```

```
#-------------------------------------------------------------------------#
% File name: #2;
% Finite difference (Explicit, Crank Nicholson) and Range
Kutta;
#-------------------------------------------------------------------------#
clear

%Input characteristic of column
dp   = 5*10^-6; %(equivalent particle diameter [m]);
L    = 0.25; %(column length [m]);
ee   = 0.3508; %(external void fraction);
ep   = 0.05; %(internal void fraction);
Di   = 4.6*10^-3;%(diameter of HPLC column [m])

%Input condition of experiment
t1   = 1200; %(run time [s] )
tp   = 4; %(time for injection [s]);
Q    = 1;%(flow rate of mobile phase[ml/min])
Q    = Q/(60*10^6);%(flow rate of mobile phase [m3/sec])
A    = pi*(Di/2)^2; %(crossectional area of column [m2)
u    = Q/(ee*A); %(interstitial velocity of mobile phase[m/s]);
uf   = 0.005; %(reference velocity[m/s]);
tal1 = t1*uf/L;%(dimensionless of time, t1);
talp = tp*uf/L;%(dimensionless of time, tp);
yf   = 0.011; %(concentration at the inlet of column);
y0   =  0; %(initial condition1);
yp0  = 0; %(initial condition2);
e    = u/uf;

%Input condition of numerical
deltal = 0.000008; %(step size of time);
i      = ceil(tal1/deltal)%(number of interval of time);
delz   = 1/2000;%(step size of distance);
j      = ceil(1/delz); %(number of interval in column);

% Set initial k, l for Runge Kutta term;
k1     =  zeros(j+1,1);
k2     =  zeros(j+1,1);
k3     =  zeros(j+1,1);
k4     =  zeros(j+1,1);
l1     =  zeros(j+1,1);
l2     =  zeros(j+1,1);
l3     =  zeros(j+1,1);
l4     =  zeros(j+1,1);

%Input parameter
K      = 5.3098; %(adsorption equilibrium [-]);
k      = 5.55*10^-5; %(mass transfer coefficient [m/s);
ap     = 6/dp; %(external surface of the adsorbent pellet
[m^2/m^3]);
Dl     =  4.3621*10^-8; %(axial dispersion coefficient[m^2/s]);
St     =   k*ap*L/uf; %(Stanton number);
Pe     =  uf*dp/Dl; %(Peclet number);

%  input initial condition
y   =  zeros(j+1,1); %(initial condition of dimensionless
condition in fluid phase);
yp  =  zeros(j+1,1) %(initial condition of dimensionless
condition in the macropore);
```

```
%Calculation of constant
A = St/(ep+(1-ep)*K);
B = dp/(Pe*L*(delz)^2);
C = -e/(2*delz);
D = -(1-ee)*St/ee;

%Runge Kutta
%t=0 to t=tp;
%Set up k l
for m = 1:ceil(talp/deltal)

  for n = 2:j
    k1(n) = deltal*(C*(y(n+1,1)-y(n-1,1))+D*(y(n,1)-yp
(n,1))+B*(y(n+1,1)-2*y(n,1)+y(n-1,1)));
    l1(n) = deltal*(A*(y(n,1)-yp(n,1)));
  end
  k1(j+1) = deltal*(D*(y(j+1,1)-yp(j+1,1))+2*B*(y(j,1)-y
(j+1,1)));
  l1(j+1) = deltal*(A*(y(j+1,1)-yp(j+1,1)));

  for n = 2:j
    k2(n) = deltal*(C*((y(n+1,1)+k1(n+1)/2)-(y(n-1,1)+k1(n-
1)/2))+D*((y(n,1)+k1(n)/2)-(yp(n,1)+l1(n)/2))+B*((y
(n+1,1)+k1(n+1)/2)-2*(y(n,1)+k1(n)/2)+(y(n-1,1)+k1(n-
1)/2)));
    l2(n) = deltal*(A*((y(n,1)+k1(n)/2)-(yp(n,1)+l1(n)/2)));
  end
  k2(j+1) = deltal*(D*((y(j+1,1)+k1(j+1)/2)-(yp(j+1,1)+l1
(j+1)/2))+2*B*((y(j,1)+k1(j)/2)-(y(j+1,1)+k1(j+1)/2)));
  l2(j+1) = deltal*(A*((y(j+1,1)+k1(j+1)/2)-(yp(j+1,1)+l1
(j+1)/2)));

  for n = 2:j
    k3(n) = deltal*(C*((y(n+1,1)+k2(n+1)/2)-(y(n-1,1)+k2(n-
1)/2))+D*((y(n,1)+k2(n)/2)-(yp(n,1)+l2(n)/2))+B*((y
(n+1,1)+k2(n+1)/2)-2*(y(n,1)+k2(n)/2)+(y(n-1,1)+k2(n-
1)/2)));
    l3(n) = deltal*(A*((y(n,1)+k2(n)/2)-(yp(n,1)+l2(n)/2)));
  end
  k3(j+1) = deltal*(D*((y(j+1,1)+k2(j+1)/2)-(yp(j+1,1)+l2
(j+1)/2))+2*B*((y(j,1)+k2(j)/2)-(y(j+1,1)+k2(j+1)/2)));
  l3(j+1) = deltal*(A*((y(j+1,1)+k2(j+1)/2)-(yp(j+1,1)+l2
(j+1)/2)));

  for n = 2:j
    k4(n) = deltal*(C*((y(n+1,1)+k3(n+1))-(y(n-1,1)+k3(n-
1)))+D*((y(n,1)+k3(n))-(yp(n,1)+l3(n)))+B*((y(n+1,1)+k3
(n+1)/2)-2*(y(n,1)+k3(n)/2)+(y(n-1,1)+k3(n-1)/2)));
    l4(n) = deltal*(A*((y(n,1)+k3(n))-(yp(n,1)+l3(n))));
  end
  k4(j+1) = deltal*(D*((y(j+1,1)+k3(j+1))-(yp(j+1,1)+l3
(j+1)))+2*B*((y(j,1)+k3(j))-(y(j+1,1)+k3(j+1))));
  l4(j+1) = deltal*(A*((y(j+1,1)+k3(j+1))-(yp(j+1,1)+l3
(j+1))));

  y(1,1) = yf;

%Calculation of dimensionless concentration at the next step of
time

for n = 2:j+1
  y(n,1) = y(n,1)+(k1(n)+2*k2(n)+2*k3(n)+k4(n))/6;
```

```
   yp(n,1)= yp(n,1)+(l1(n)+2*l2(n)+2*l3(n)+l4(n))/6;
end
if rem(m,100) == 0
   yexit(m/100,1) = y(j+1,1);
end
if floor(m/1000)==ceil(m/1000)
   fprintf('m=%f \n',m);
   yexit(m/100,1)
   y(1000,1)
   y(2000,1)
   y(4000,1)
end

end

%Runge Kutta
%At t=tp to t=t1;

y(1,1) = 0;
for m = ceil(talp/deltal)+1:ceil(tal1/deltal)
%for m = 1:2
   for n = 2:j
      k1(n) = deltal*(C*(y(n+1,1)-y(n-1,1))+D*(y(n,1)-yp
(n,1))+B*(y(n+1,1)-2*y(n,1)+y(n-1,1)));
      l1(n) = deltal*(A*(y(n,1)-yp(n,1)));
   end
   k1(j+1) = deltal*(D*(y(j+1,1)-yp(j+1,1))+2*B*(y(j,1)-y
(j+1,1)));
   l1(j+1) = deltal*(A*(y(j+1,1)-yp(j+1,1)));

   for n = 2:j
      k2(n) = deltal*(C*((y(n+1,1)+k1(n+1)/2)-(y(n-1,1)+k1(n-
1)/2))+D*((y(n,1)+k1(n)/2)-(yp(n,1)+l1(n)/2))+B*((y
(n+1,1)+k1(n+1)/2)-2*(y(n,1)+k1(n)/2)+(y(n-1,1)+k1(n-
1)/2)));
      l2(n) = deltal*(A*((y(n,1)+k1(n)/2)-(yp(n,1)+l1(n)/2)));
   end
   k2(j+1) = deltal*(D*((y(j+1,1)+k1(j+1)/2)-(yp(j+1,1)+l1
(j+1)/2))+2*B*((y(j,1)+k1(j)/2)-(y(j+1,1)+k1(j+1)/2)));
   l2(j+1) = deltal*(A*((y(j+1,1)+k1(j+1)/2)-(yp(j+1,1)+l1
(j+1)/2)));

   for n = 2:j
      k3(n) = deltal*(C*((y(n+1,1)+k2(n+1)/2)-(y(n-1,1)+k2(n-
1)/2))+D*((y(n,1)+k2(n)/2)-(yp(n,1)+l2(n)/2))+B*((y
(n+1,1)+k2(n+1)/2)-2*(y(n,1)+k2(n)/2)+(y(n-1,1)+k2(n-
1)/2)));
      l3(n) = deltal*(A*((y(n,1)+k2(n)/2)-(yp(n,1)+l2(n)/2)));
   end
   k3(j+1) = deltal*(D*((y(j+1,1)+k2(j+1)/2)-(yp(j+1,1)+l2
(j+1)/2))+2*B*((y(j,1)+k2(j)/2)-(y(j+1,1)+k2(j+1)/2)));
   l3(j+1) = deltal*(A*((y(j+1,1)+k2(j+1)/2)-(yp(j+1,1)+l2
(j+1)/2)));

   for n = 2:j
      k4(n) = deltal*(C*((y(n+1,1)+k3(n+1))-(y(n-1,1)+k3(n-
1)))+D*((y(n,1)+k3(n))-(yp(n,1)+l3(n)))+B*((y(n+1,1)+k3
(n+1)/2)-2*(y(n,1)+k3(n)/2)+(y(n-1,1)+k3(n-1)/2)));
      l4(n) = deltal*(A*((y(n,1)+k3(n))-(yp(n,1)+l3(n))));
   end
   k4(j+1) = deltal*(D*((y(j+1,1)+k3(j+1))-(yp(j+1,1)+l3
(j+1)))+2*B*((y(j,1)+k3(j))-(y(j+1,1)+k3(j+1))));
```

```
   l4(j+1) = deltal*(A*((y(j+1,1)+k3(j+1))-(yp(j+1,1)+l3
(j+1))));

% Calculation of dimensionless concentration at the next step
of time

   y(1,1) = 0;
for n = 2:j+1
   y(n,1) = y(n,1)+(k1(n)+2*k2(n)+2*k3(n)+k4(n))/6;
   yp(n,1)= yp(n,1)+(l1(n)+2*l2(n)+2*l3(n)+l4(n))/6;
end
if rem(m,100) == 0
   yexit(m/100,1) = y(j+1,1);
end
if floor(m/1000)==ceil(m/1000)
   fprintf('m=%f \n',m);
   yexit(m/100,1)
   y(1000,1)
   y(2000,1)
   y(4000,1)
end
end
```

Appendix B

The Extraction of Soybean Flake and Pre-Purification

1. One kilogram of defatted-soybean flakes (obtained from Aun food industry) is extracted by 80% aqueous etanol at 75°C for a period of 100 minutes.
2. The extracted solution is then filtered through a filtration paper
3. The extracted solution is subjected to a vacuum evaporation unit to remove all of ethanol and kept in a refrigerator at 0°C

BIOGRAPHY

Ms. Nattada Junghuttakarnsatit was born on 4th March, 1979 in Bangkok. She finished her higher secondary course from Triamudomsuksa School in May 1997. Later on, she studied in the Major of Chemical Engineering in Faculty of Engineering at Chulalongkorn University. She participated in the Biochemical Engineering research group and achieved her Master's degree in October 2002.